INTERIOR NOISE REDUCTION BY ALTERNATE RESONANCE TUNING

SIX MONTH PROGRESS REPORT

Prepared for: Structural Acoustics Branch
NASA Langley Research Center

Prepared by: Donald B. Bliss
James A. Gottwald
Jeffrey W. Bryce

Department of Mechanical Engineering
and Materials Science
Duke University
Durham, North Carolina 27706

August 1987

1. INTRODUCTION

Existing interior noise reduction techniques for aircraft fuselages perform reasonably well at higher frequencies, but are inadequate at low frequencies, particularly with respect to the low blade passage harmonics with high forcing levels found in propeller aircraft. A method is being studied which considers aircraft fuselages lined with panels alternately tuned to frequencies above and below the frequency that must be attenuated. Adjacent panels would oscillate at equal amplitude, to give equal acoustic source strength, but with opposite phase. Provided these adjacent panels are acoustically compact, the resulting cancellation causes the interior acoustic modes to be cut off, and therefore be non-propagating and evanescent. This interior noise reduction method, called Alternate Resonance Tuning (ART), is currently being investigated theoretically and experimentally. This new concept has potential application to reducing interior noise due to the propellers in advanced turboprop aircraft as well as for existing aircraft configurations.

The ART technique is a procedure intended to reduce low frequency noise within an aircraft fuselage. A fuselage wall could be constructed of, or lined with, a series of special panels which would allow the designer to control the wavenumber spectrum of the wall motion, thus controlling the interior sound field. By judicious tuning of the structural response of individual panels, wavelengths in the fuselage wall can be reduced to the order of the panel size, thus causing low frequency interior acoustic modes to be cut off provided these panels are sufficiently small. By cutting off the acoustic modes in this manner, a significant reduction of interior noise at the propeller blade passage harmonics should be achieved.

Current noise control treatments have already demonstrated that the mass

and stiffness of individual fuselage panels can be altered. It seems reasonable, therefore, that panel resonant frequencies can be manipulated to achieve the ART effect. Application of this concept might involve the modification of existing structural panels or development of a new design for fuselage interior trim panels. Although complete acoustic cut-off will not be achievable in practice, an approximate cancellation should still substantially reduce interior noise levels at the particular frequency of interest. It is important to note that the ART method utilizes the flexibility and dynamic behavior of the structure to good advantage, although these properties are not normally beneficial in noise control.

This progress report summarizes the work carried out at Duke University during the first 6 months of a contract supported by the Structural Acoustics Branch at NASA Langley. Considerable progress has been made both theoretically and experimentally as described in the following sections. It is important to note that all the work carried out so far indicates that the ART concept is indeed capable of achieving a significant reduction in the sound transmission through flexible walls.

2. THEORETICAL ANALYSIS

2.1 Model Problem

The theoretical model currently being developed involves sound transmission through a wall of panels. The wall is of infinite extent and is composed of idealized spring-mass-damper panels arranged in a periodic pattern. Sound waves strike the wall at normal incidence and the acoustic transmission is calculated in terms of the dynamic properties of the panels. Beyond the panel wall the analysis allows for the placement of a parallel barrier wall of specified impedance to simulate reflections within an enclosure. The configuration being analyzed is shown in Figure 1a. The panel wall is subdivided into identical blocks of panels. Within each block the current analysis allows there to be four rectangular panels of identical shape, but each of these can have different dynamic properties. In general, a system of n panels will be capable of (n-1) ART cancellation frequencies. Figure 1b shows a cross section through the wall with two of the four distinct panel sections shown; also note the reflection wall condition with variable impedance z_b. By adjusting the panel dimensions and choosing different dynamical properties, a variety of 1-D, 2-D, and 3-D physical configurations can be simulated. Figure 2 summarizes the configuration possibilities. This analysis applies not only to an infinite wall of panels, but it is also equivalent to placing up to four different panels in a rectangular duct, as shown in Figure 3. The latter scheme is the experimental configuration which will be described in Section 3.

2.2 Analysis Methods

The panel wall model problem is equivalent to a problem of sound transmission through panels in a duct, where the wavelength must be large compared to the duct cross-sectional dimensions to achieve the acoustic

cut-off required by the Alternate Resonance Tuning (ART) concept. Under these conditions, the sound transmission can be analyzed by a quasi one-dimensional treatment utilizing an acoustic branch analysis, or acoustic circuit analysis. This approach provides relatively simple results with which the more elaborate analysis, described below can be checked. The acoustic loading due to cut-off modes (inertance or apparent mass effects) acting on the panels is neglected in such an analysis. Essentially, the incident acoustic field is split into separate branches, one for each panel, and these branches are rejoined on the other side of the wall. At each branch junction pressure and flow continuity conditions are applied.

Figure 4 shows the hypothetical configuration used in the branch analysis. From this analysis we may solve for the ratio of transmitted to incident pressure as

$$\frac{p^{BT}}{p^{AI}} = \left(\frac{z_o + \rho_o c}{z_b}\right)\left(\frac{z_o^B}{z_o^A + \rho_o c}\right) \qquad (1)$$

$$\text{where } z_o^A = z_o^B + \frac{S_A}{\sum_{i=1}^{N} \frac{S_i^2}{Z_{mi}}}$$

$$\text{and } S_A = S_B = \sum_{i=1}^{\infty} S_i$$

where z_o^A is the impedance on the left hand side of the panel assembly, and z_o^B is the acoustic impedance on the right hand side of the duct looking downstream toward the termination impedance z_b. The quantity Z_{mi} is the mechanical impedance of the ith panel and S_i is the area of this panel. The result (1) above may be generalized for any number of panels. For two panels and an anechoic termination, we obtain

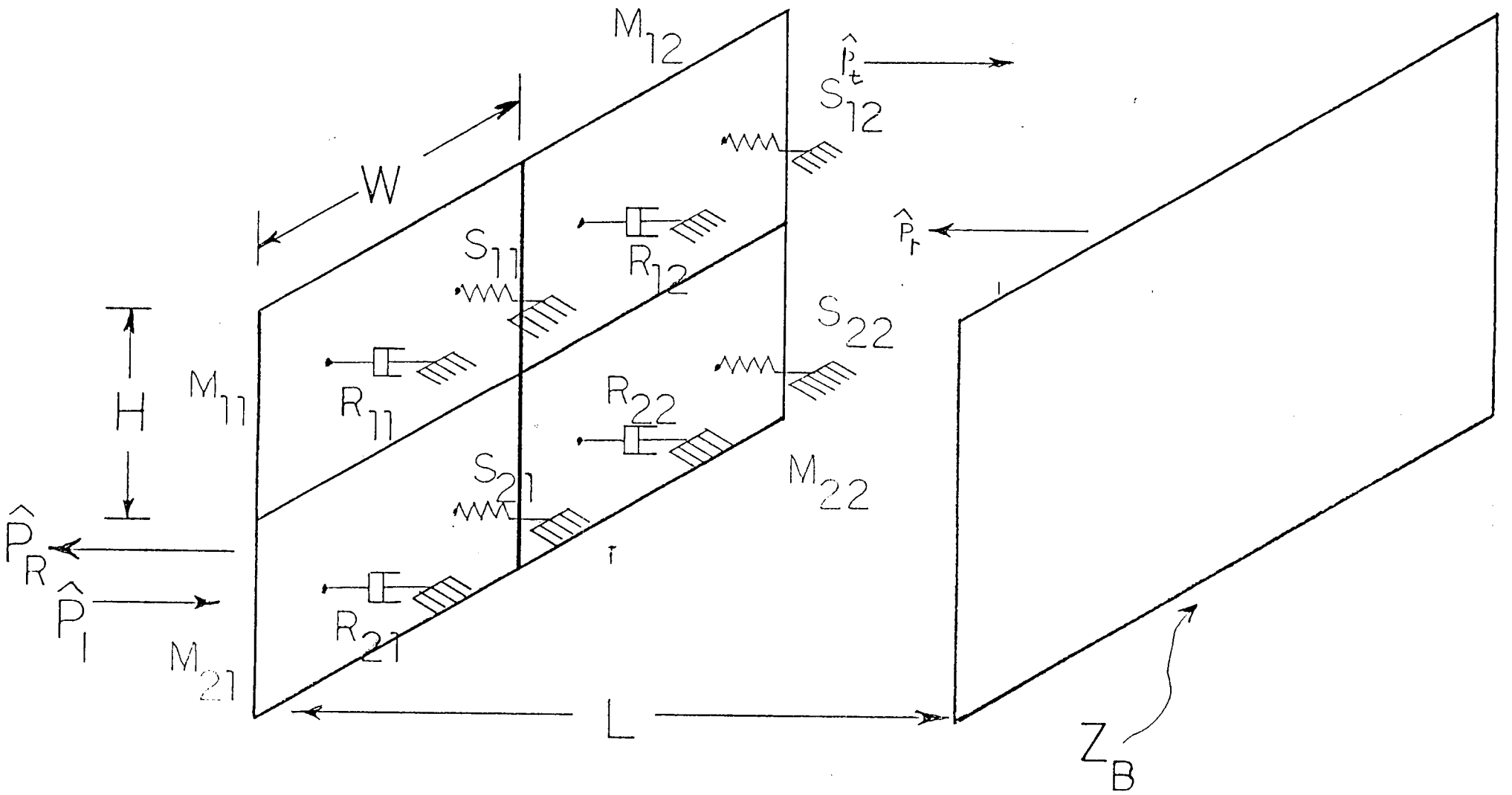

FIGURE 1a: Schematic of Theoretical Analysis Configuration

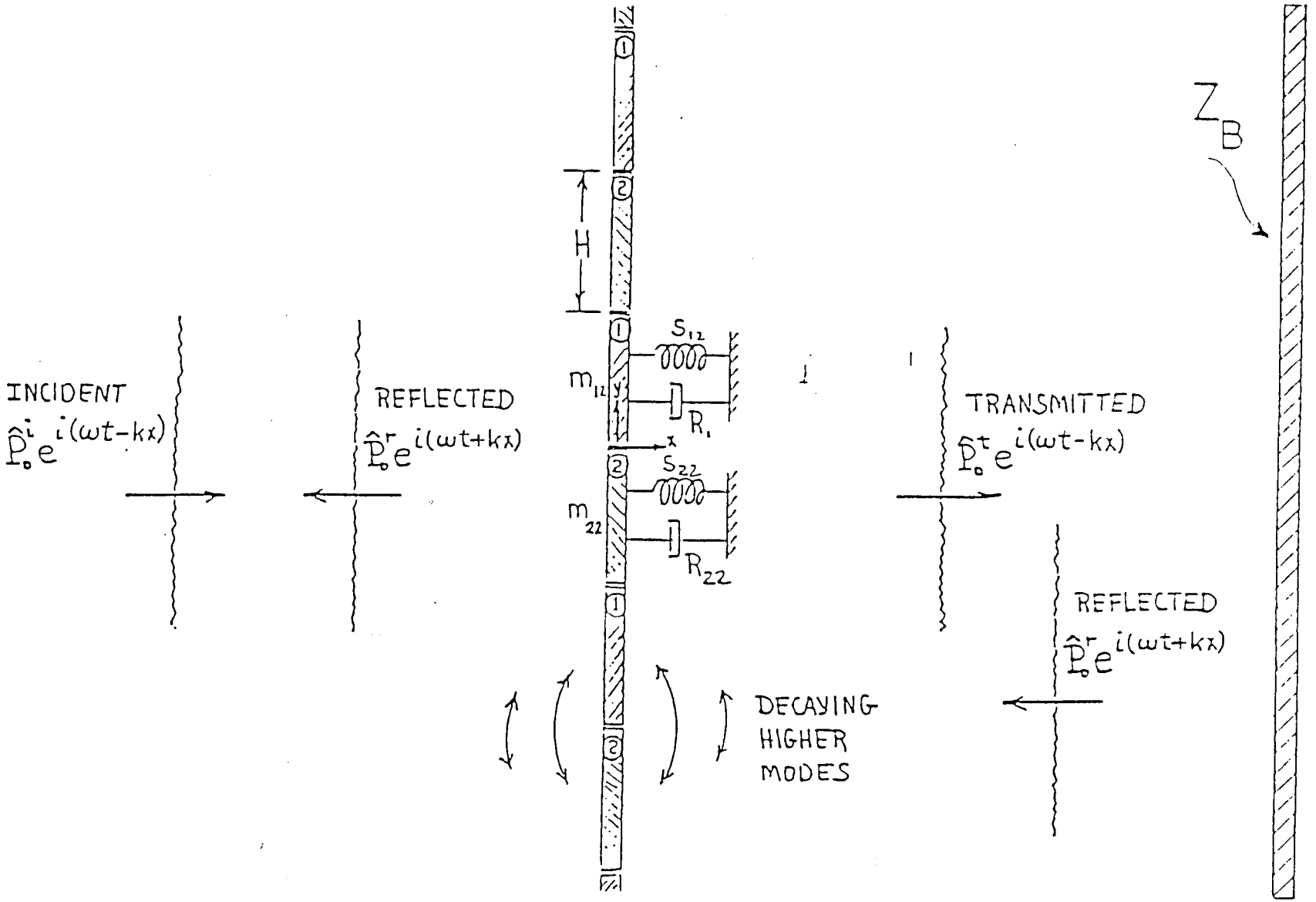

FIGURE 1b: Cross Section Through Panel Wall

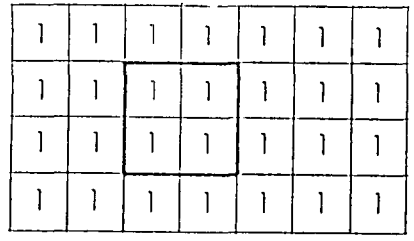

1-D

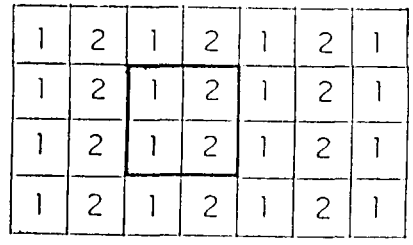

2-D

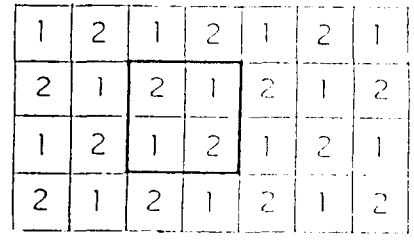

DIAGONAL

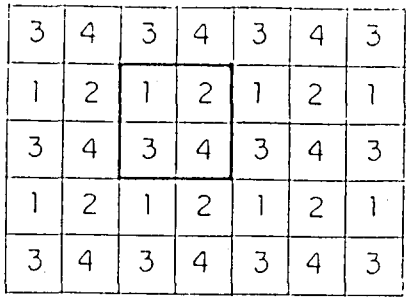

3-D

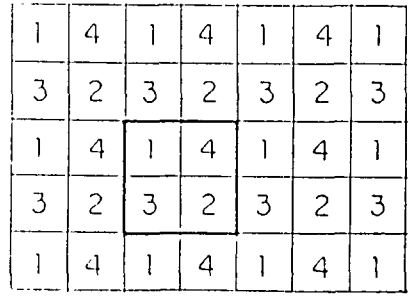

3-D (alternate 1)

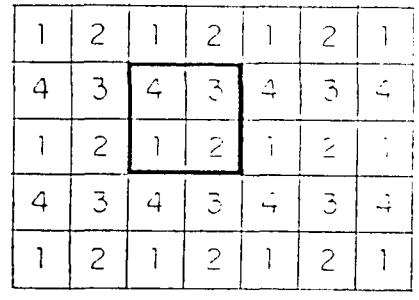

3-D (alternate 2)

FIGURE 2: FOUR PANEL CONFIGURATION POSSIBILITIES

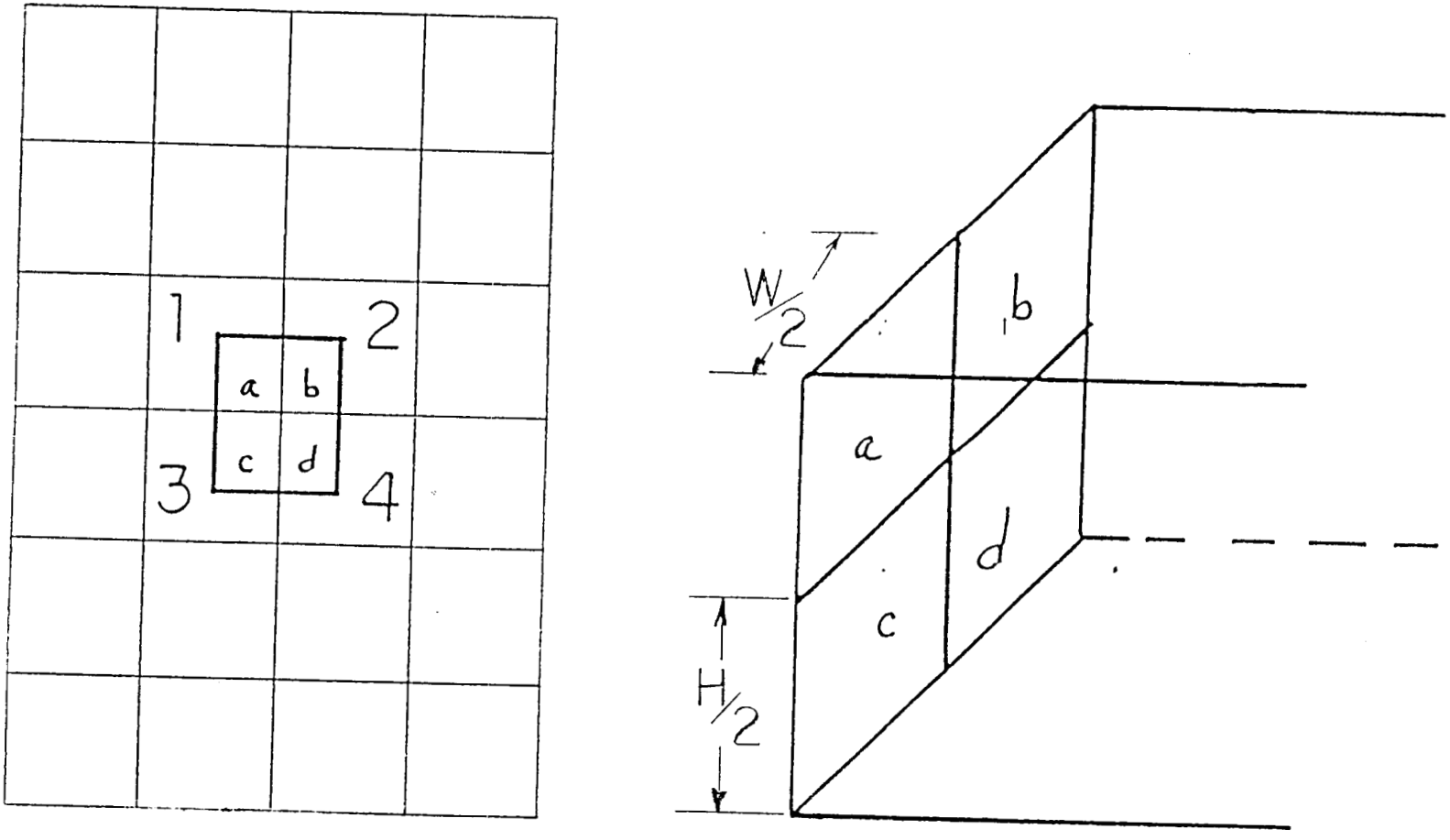

FIGURE 3: DIRECT EQUIVALENT OF TYPICAL FOUR PANEL ARRAY TRANSFERRED TO EXPERIMENTAL DUCT

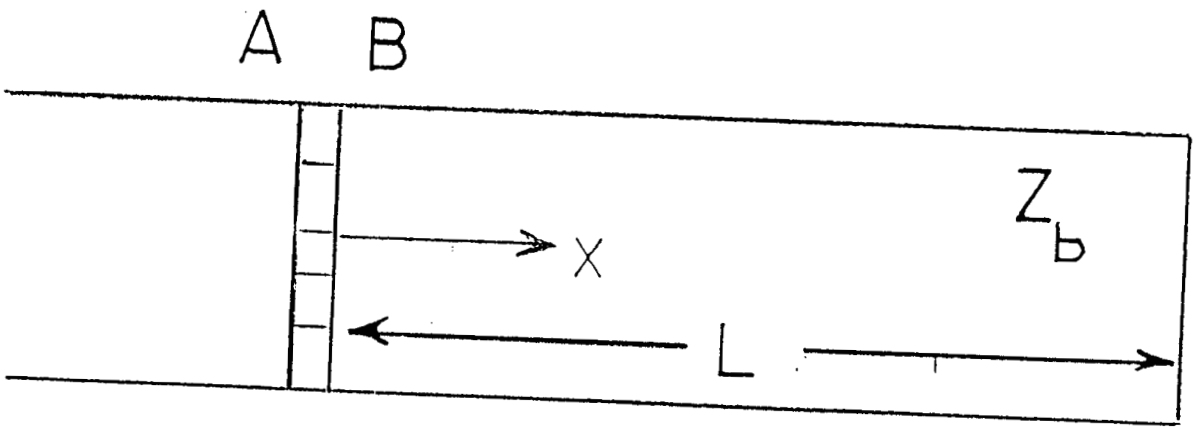

FIGURE 4: Configuration of Branch Analysis

$$\frac{p^{BT}}{p^{AI}} = \frac{Z_{m_1} + Z_{m_2}}{Z_{m_2} + \frac{2}{\rho_o c S_A} Z_{m_1} Z_{m_2}}$$

For a four panel model,

$$\frac{p^{BT}}{p^{AI}} = \frac{Z_{m_1}Z_{m_2}Z_{m_3} + Z_{m_2}Z_{m_3}Z_{m_4} + Z_{m_3}Z_{m_4}Z_{m_1} + Z_{m_4}Z_{m_1}Z_{m_2}}{Z_{m_1}Z_{m_2}Z_{m_3} + Z_{m_2}Z_{m_3}Z_{m_4} + Z_{m_3}Z_{m_4}Z_{m_1} + Z_{m_4}Z_{m_1}Z_{m_2} + \frac{8}{\rho_o c S_A} Z_{m_1}Z_{m_2}Z_{m_3}Z_{m_4}}$$

The full three-dimensional acoustic solution of the configuration shown in Figure 1a has also been derived. This problem satisfies the linearized wave equation

$$\frac{\partial^2 p}{\partial x^2} + \frac{\partial^2 p}{\partial y^2} + \frac{\partial^2 p}{\partial z^2} - \frac{1}{c^2}\frac{\partial^2 p}{\partial t^2} = 0$$

The pressure field on the incident (external) side of the panel array is given by

$$\begin{aligned} p_{ex}(x,y,z,t) = {} & \hat{P}^I_{oo}\, e^{i(\omega t - kx)} + \hat{P}^R_{oo}\, e^{i(\omega t + kx)} \\ & + \sum_{m=1}^{\infty}\sum_{n=1}^{\infty} \hat{P}^R_{mn}\, e^{i\omega t} e^{\hat{\beta}x} \cos\left(\frac{2m\pi}{W}\right)y \cos\left(\frac{2n\pi}{H}\right)z \\ & + \sum_{m=1}^{\infty}\sum_{n=1}^{\infty} \tilde{P}^R_{mn}\, e^{i\omega t} e^{\tilde{\beta}x} \sin\left[\frac{(2m-1)\pi}{W}\right]y \sin\left[\frac{(2n-1)\pi}{H}\right]z \\ & + \sum_{m=0}^{\infty}\sum_{n=1}^{\infty} \hat{\tilde{P}}^R_{mn}\, e^{i\omega t} e^{\hat{\tilde{\beta}}x} \cos\left(\frac{2m\pi}{W}\right)y \sin\left[\frac{(2n-1)\pi}{H}\right]z \\ & + \sum_{m=1}^{\infty}\sum_{n=0}^{\infty} \tilde{\hat{P}}^R_{mn}\, e^{i\omega t} e^{\tilde{\hat{\beta}}x} \sin\left[\frac{(2m-1)\pi}{W}\right]y \cos\left(\frac{2n\pi}{H}\right)z \end{aligned} \qquad (2)$$

where the superscripts I,R denote exterior incident and reflected waves, respectively. The quantities $\hat{P}_{mn}$ and $\tilde{P}_{mn}$ are the acoustic modal amplitudes and

$$\hat{\beta} = \left[\left(\frac{2m\pi}{W}\right)^2 + \left(\frac{2n\pi}{H}\right)^2 - k^2\right]^{1/2}$$

$$\tilde{\beta} = \left[\left(\frac{(2m-1)\pi}{W}\right)^2 + \left(\frac{(2n-1)\pi}{H}\right)^2 - k^2\right]^{1/2}$$

$$\hat{\beta}\tilde{} = \left[\left(\frac{2m\pi}{W}\right)^2 + \left(\frac{(2n-1)\pi}{H}\right)^2 - k^2\right]^{1/2} \qquad (3)$$

$$\tilde{\beta}\hat{} = \left[\left(\frac{(2m-1)\pi}{W}\right)^2 + \left(\frac{2n\pi}{H}\right)^2 - k^2\right]^{1/2} .$$

The above β are real valued because the panel size is assumed sufficiently small to satisfy the cutoff conditions

$$\frac{\omega H}{c} < \frac{\pi}{2}$$

$$\frac{\omega W}{c} < \frac{\pi}{2}$$

Thus the higher modes in (2) above decay exponentially away from the panel array. A similar general solution can be shown to apply to the pressure field on the transmitted (internal) side of the panel array. In the latter case, however, the various β are negative quantities, and a transmitted pressure wave and a reflected pressure wave (from the reflecting wall) are included. An impedance relation of the form

$$\frac{\hat{p}^r_{oo}}{\hat{p}^t_{oo}} = e^{-i2kL}\left(\frac{z_b - \rho_o c}{z_b + \rho_o c}\right) \qquad (4)$$

may be used to express the reflected wave (off the interior barrier) in terms of the transmitted wave. Note that here t and r denote the pressure wave transmitted through the panel array and reflected from the interior barrier, respectively. Higher order modes are again assumed to decay, due to acoustic cut-off.

The panels are then represented in terms of their mechanical impedances

$$Z_{ij} = R_{ij} + i(m_{ij}\omega - s_{ij/\omega}) \qquad (5)$$

where R_{ij} are the damping values, m_{ij} are the individual panel masses, and s_{ij} are the panel spring constants. Here the subscripts ij denote the panels shown in Figure 1a. Using the impedance relations, the panel forces are calculated as

$$F_{ij}e^{i\omega t} = Z_{ij}U_{ij}e^{i\omega t}$$

where F_{ij} is the net force on each panel obtained by integrating equation (2) over each panel area, and U_{ij} are the individual panel velocities. An additional continuity equation of the form

$$\frac{1}{4}\sum_{i=1}^{\bar{2}}\sum_{j=1}^{2} U_{ij} = \frac{1}{\rho_o c}\left(\hat{p}^t_{oo} - \hat{p}^r_{oo}\right)$$

coupled with the impedance relation (5) completes a set of five equations and five unknowns (4 velocities and the transmitted pressure wave P^t_{oo}). This system of linear equations with complex coefficients is appropriately non-dimensionalized and solved numerically using standard solution techniques.

Figures 5-7 show representative theoretical results for the four panel model discussed above. In these figures the transmission loss is based on the ratio of rms pressure on the incident side wall to rms pressure measured at the reflecting wall. The frequency is nondimensionalized by either the panel resonant frequency for identical panel cases, or the by lowest ART cancellation frequency. Figures 5a-e show a series of results for a two panel system. This is essentially a 2-D panel configuration as shown in Figure 2. These results were achieved by assuming a typical damping ratio for an aircraft panel ($\zeta = .05$) and an anechoic termination with $z_b = \rho_o c$. Figure 5a shows a transmission loss calculation for identical panels (actually audio speakers in the experimental setup; see Section 3) with resonance at

FIGURE 5A
TRANSMISSION LOSS FOR IDENTICAL PANELS
RESONANCE SET AT 1.0 WITH ANECHOIC TERMINATION

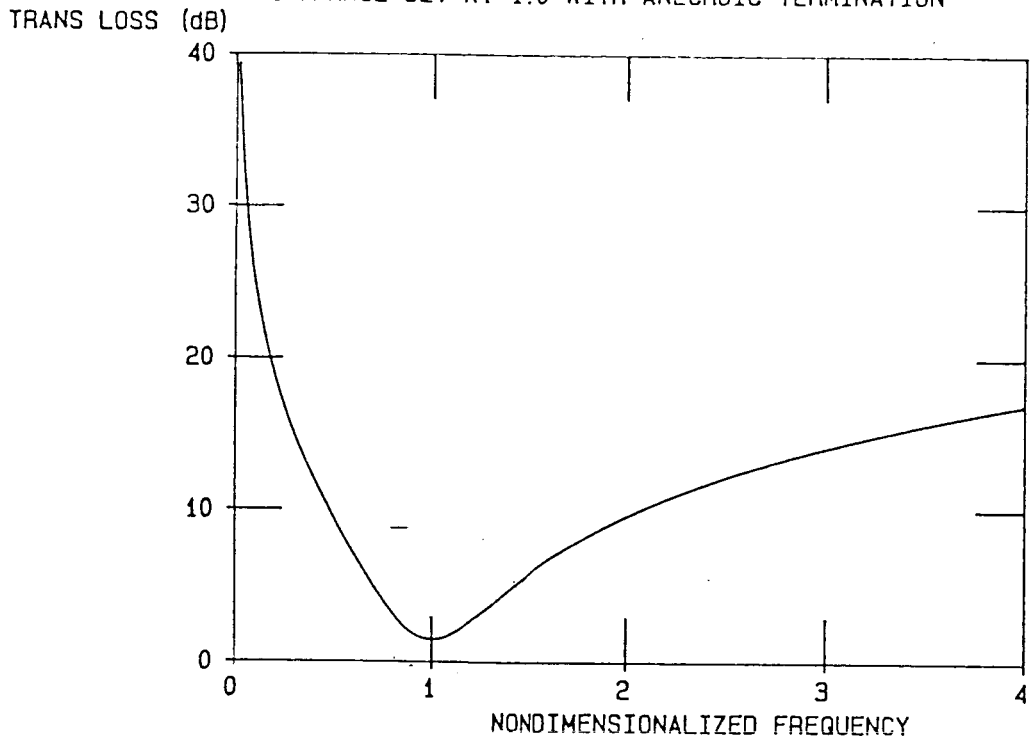

FIGURE 5B
TRANSMISSION LOSS ACROSS ART PANELS IN THE TWO
PANEL DUCT WITH RESONANCE SET AT 0.5 AND 1.5
AND ANECHOIC TERMINATION

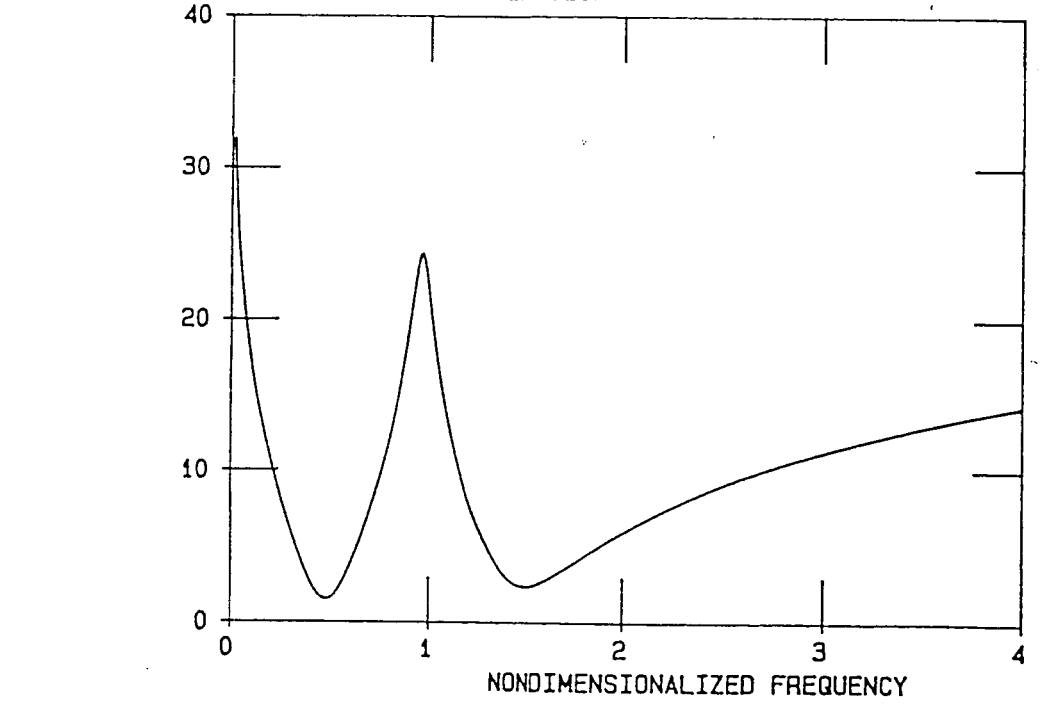

FIGURE 5C
TRANSMISSION LOSS DIFFERENCE BETWEEN ART PANELS AND IDENTICAL PANELS FOR THE TWO PANEL DUCT WITH ANECHOIC TERMINATION

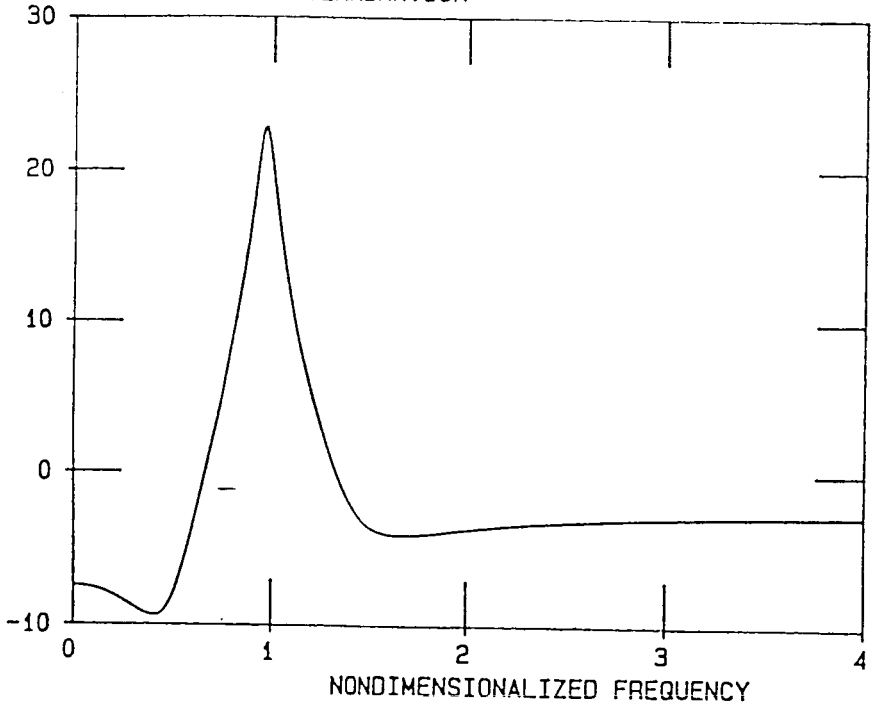

FIGURE 5D
TRANSMISSION LOSS AVERAGE FOR THE ANECHOIC TWO PANEL DUCT

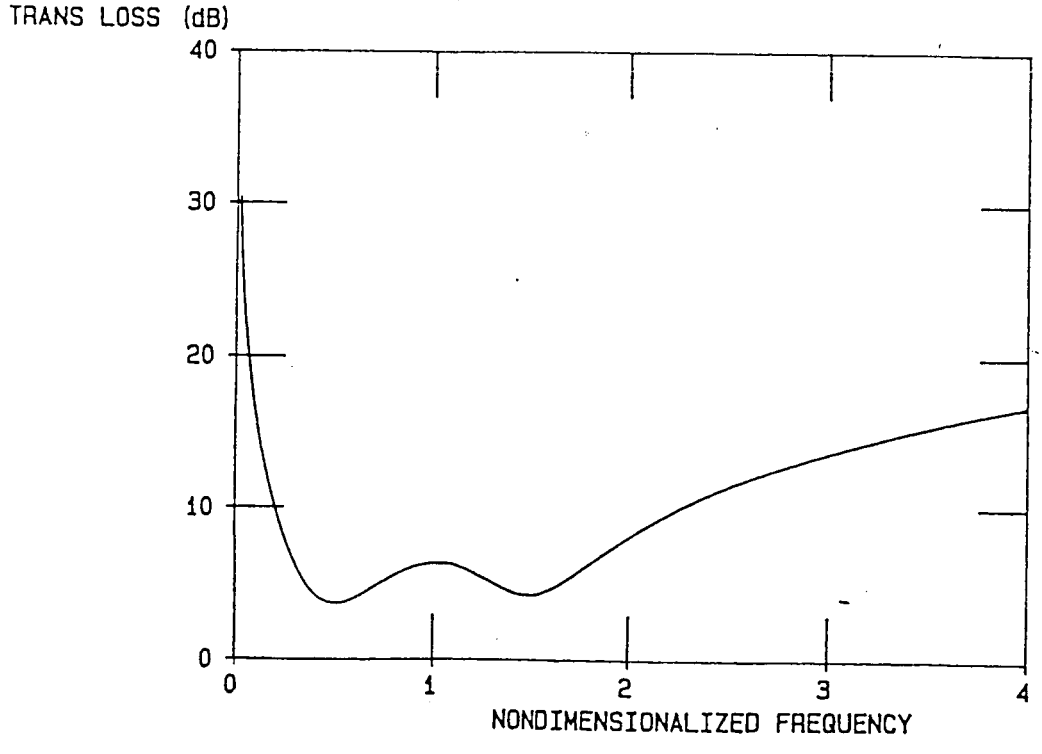

FIGURE 5E
DIFFERENCE BETWEEN ART AND TRANSMISSION LOSS
AVERAGE CALCULATION FOR THE ANECHOIC CASE

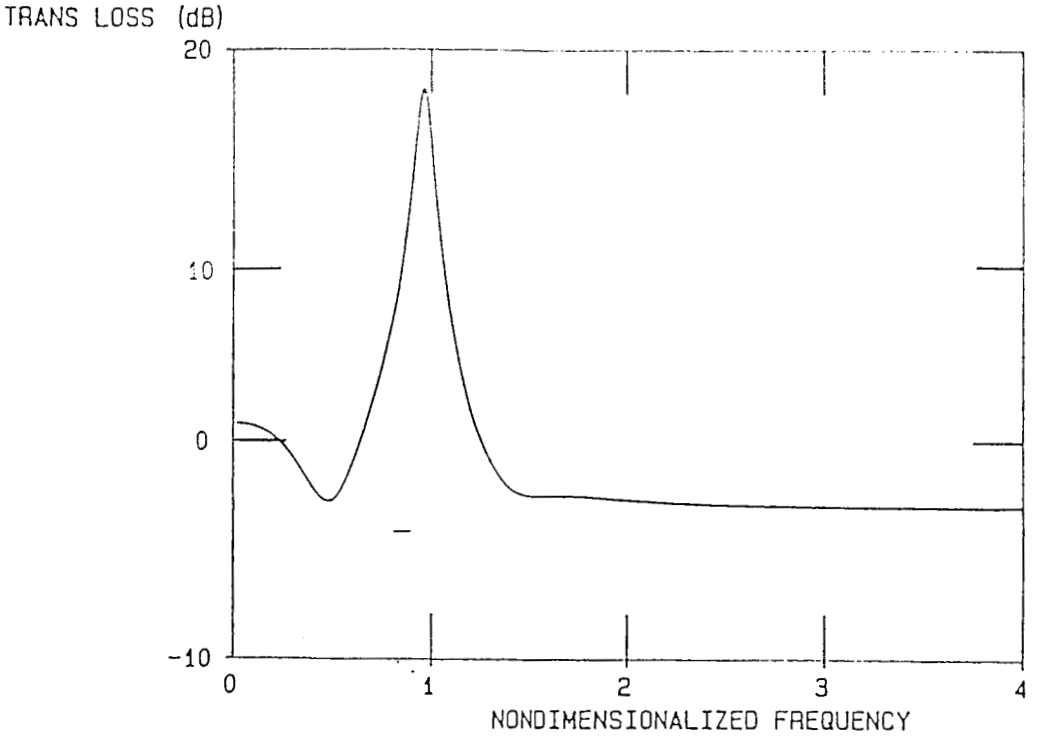

nondimensional frequency equal to 1. There is still a small transmission loss at resonance due to system damping. At higher frequencies the transmission loss is mass dominated and increases at 6dB per octave. Figure 5b shows transmission loss with ART panels. Here the panels have resonances at nondimensional frequencies of .5 and 1.5. Note approximately 24 dB of transmission loss at the design frequency. Figure 5c plots the difference between ART panels and identical panels.

Figure 5d shows the average transmission loss for the identical panel case using results from two simulations having all panels with resonant frequencies at either .5 or 1.5. These results are averaged using an average transmission loss as calculated from the formula

$$TL_{AVG} = 10\log_{10}(n) - 10\log\left(\sum_{i=1}^{n} 10^{(-TL_i/10)}\right) \qquad (6)$$

where n is the total number of panels considered in the model (currently 1 to 4) and the subscript denotes the ith panel. In this manner, the ART calculations are compared to cases where similar panels are utilized, but the acoustic fields from these panels do not interact. Figure 5e shows the difference between the ART transmission loss and the average transmission loss calculations. Presenting the results in this manner shows the true ART contribution to noise reduction.

Figure 6 shows a similar sequence as described above, except now a four panel model with four natural frequencies of 0.5, 1.5, 2.5, and 3.5 is assumed. Again, a damping ratio of $\zeta = .05$ was assumed. Ratios of panel masses (a necessary element in the calculation) were derived from a simple case assuming no damping and no apparent mass. The reflection wall impedance is again taken as $\rho_0 c$. This combination of system parameters should yield cancellation at non-dimensionalized frequencies of 1.0, 2.0, and 3.0.

FIGURE 6A
TRANSMISSION LOSS FOR IDENTICAL PANELS IN THE FOUR PANEL DUCT
RESONANCES SET AT 2.0 WITH ANECHOIC TERMINATION

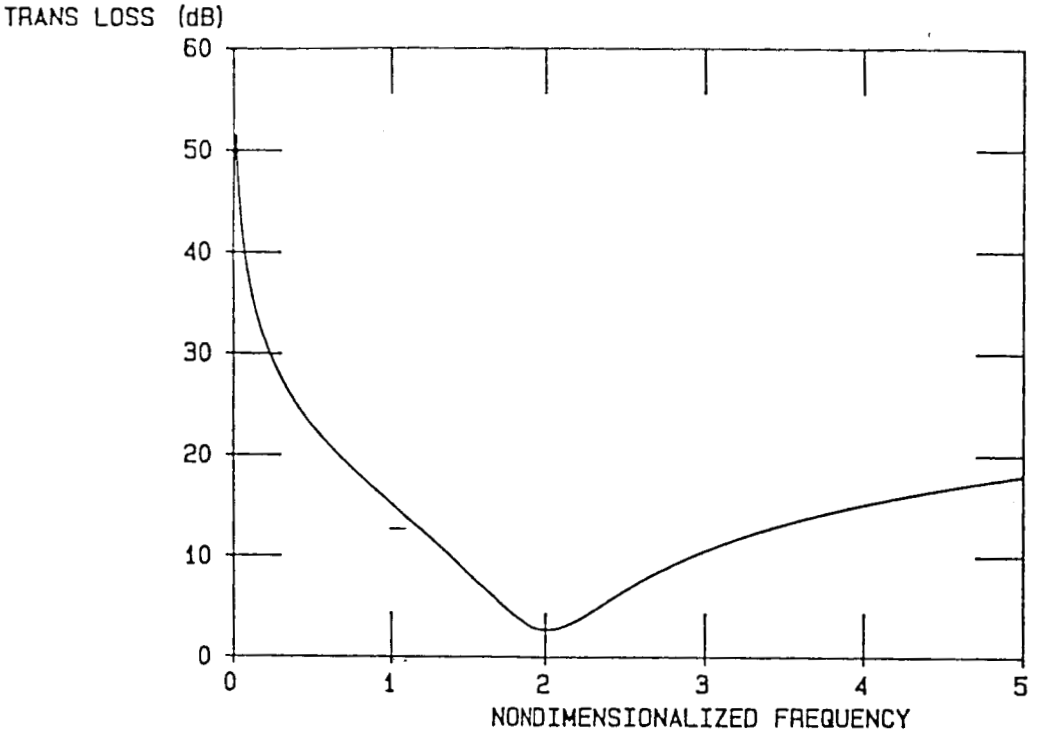

FIGURE 6B
TRANSMISSION LOSS ACROSS ART PANELS IN THE
FOUR PANEL DUCT WITH RESONANCES AT .5, 1.5,
2.5, AND 3.5 AND ANECHOIC TERMINATION

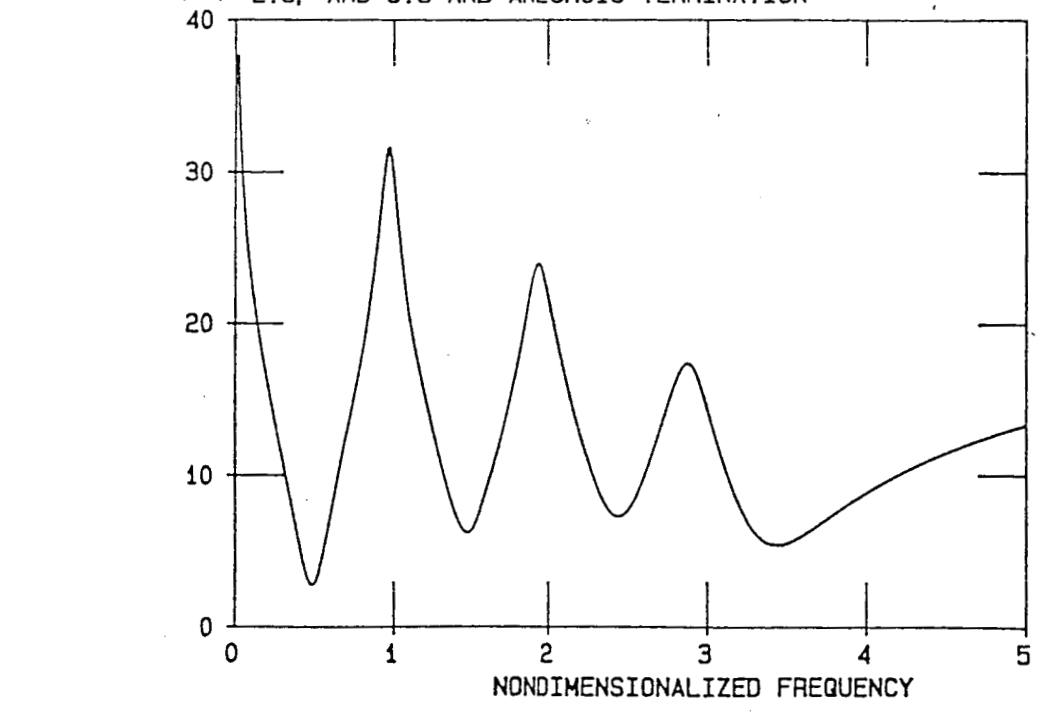

FIGURE 6C
TRANSMISSION LOSS DIFFERENCE BETWEEN ART PANELS AND IDENTICAL PANELS FOR FOUR PANEL DUCT WITH ANECHOIC TERMINATION

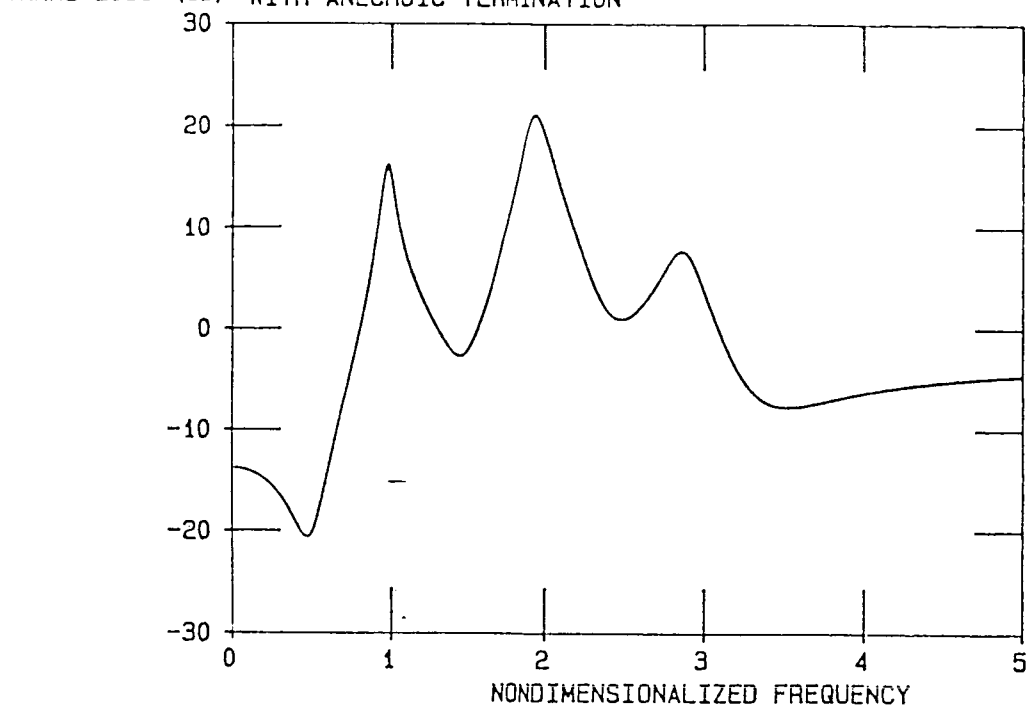

FIGURE 6D
TRANSMISSION LOSS AVERAGE FOR ANECHOIC FOUR PANEL DUCT

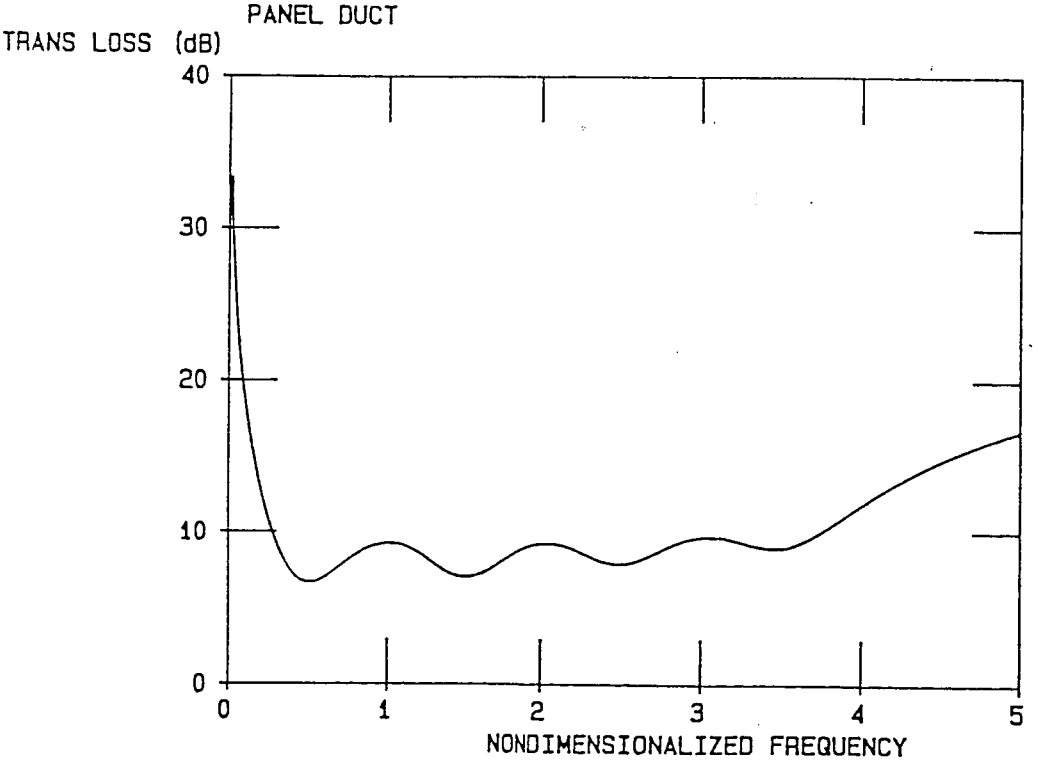

FIGURE 6E
DIFFERENCE BETWEEN ART AND TRANSMISSION LOSS
AVERAGE CALCULATION FOR ANECHOIC CASE

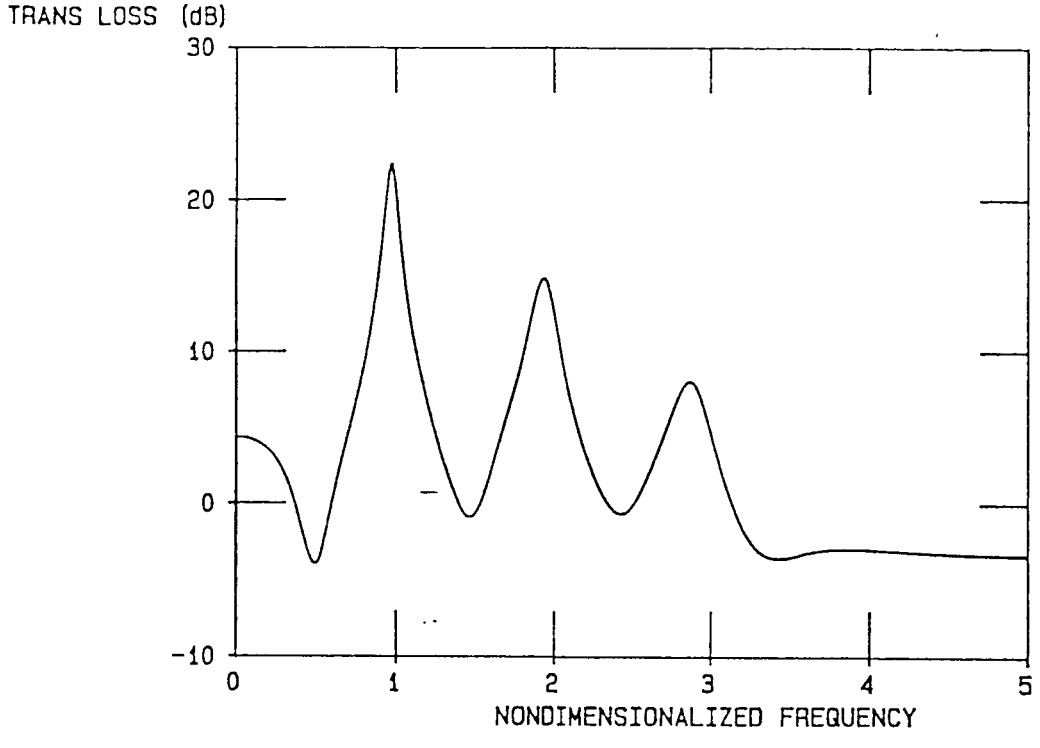

However, the actual cancellation frequencies are slightly different because the mass ratios were taken from a no damping, no apparent mass case. Work is in progress on a computation method to determine ratios of panel masses for the general case. However, Figure 6e still indicates losses of 23 dB, 16 dB, and 8 dB at the actual cancellation frequencies.

Figures 7a and 7b are transmission loss calculations using an interior wall reflection condition based on acoustic modal damping in aircraft interiors, $\zeta = .025$ to $.05$, as quoted in the literature. In the present model problem this corresponds to a reflecting wall absorption coefficient α_A in the range

$$.3 < \alpha_A < .6$$

where

$$\alpha_A = \frac{4\rho_o c\, r_b}{(r + \rho_o c)^2 + x_b^2} \tag{7}$$

and the reflecting wall impedance is

$$z_b = r_b + ix_b$$

If we assume z_b is totally resistive, i.e., $x_b = 0$, we may solve for an approximate range of z_b from equation (7) above as

$$4.4 < z_b < 11.2 \tag{8}$$

Figures 7a and 7b represent a four panel model with reflecting wall impedances at the upper and lower bounds of equation (8) above. The model predicts attenuation of between 15 dB and 22 dB at the cancellation frequencies in these cases.

For effective use of the ART technique, panel oscillations must be out of phase with equal amplitudes. Figure 8 shows a transmission loss where the damping ratio is $\zeta = .01$. This plot is the equivalent of Figure 6b with less damping. Clearly when motions are more perfectly out of phase (achieved here

FIGURE 7A
TRANSMISSION LOSS ACROSS ART SPEAKERS
RESONANCES AT .5, 1.5, 2.5, AND 3.5
REFLECTING WALL NORMALIZED IMPEDANCE = 11.2 (α=0.3)

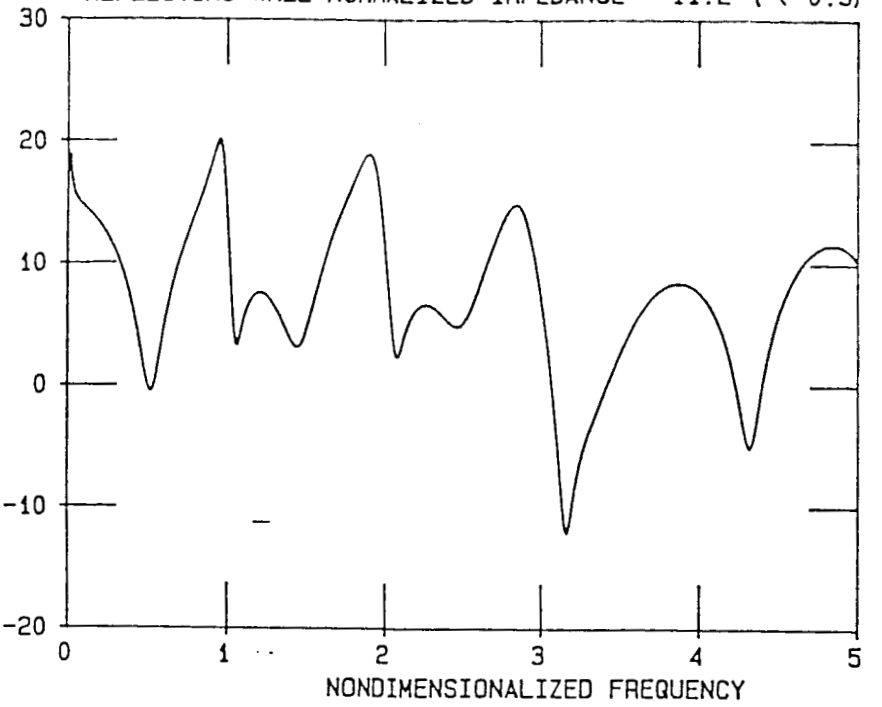

FIGURE 7B
TRANSMISSION LOSS ACROSS ART PANELS
RESONANCES AT .5, 1.5, 2.5, AND 3.5
REFLECTING WALL NORMALIZED IMPEDANCE = 4.4 (α=0.6)

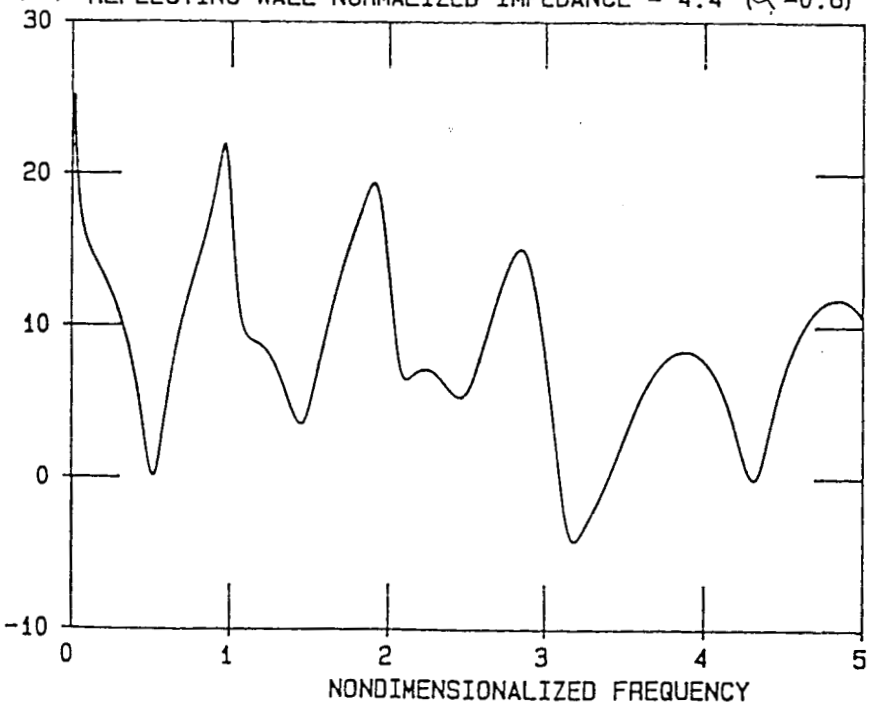

by reducing the damping), more attenuation can be achieved. Figure 8 shows transmission losses between 30 dB and 45 dB for this case. In the next six months, more analysis will be done to determine the appropriate system parameters to achieve a better out of phase condition at equal amplitudes. One way to achieve the out-of-phase condition may be to use a double panel model, as shown in Figure 9. Essentially each panel in the four panel model would be replaced by a double spring-mass-damper system. The general analysis for this case is complete, but a method of determining the proper mass relationships among the panels to achieve the ART effect is yet to be developed. Analysis of the general four panel model on a flexible frame is another case under consideration, and analytic work has just begun on that topic. Longer term analysis goals include beginning work on modeling the aircraft fuselage as a 3-D acoustic enclosure and analysis of the effect of a generalized external pressure field. In particular, the latter area will deal with the high trace speed of propagating disturbances caused by propeller rotation.

FIGURE 8
FOUR PANEL MODEL WITH REDUCED DAMPING TO ACHIEVE
MORE NEARLY OUT OF PHASE CONDITION
RESONANCES AT .5, 1.5, 2.5, AND 3.5 WITH ANECHOIC TERMINATION

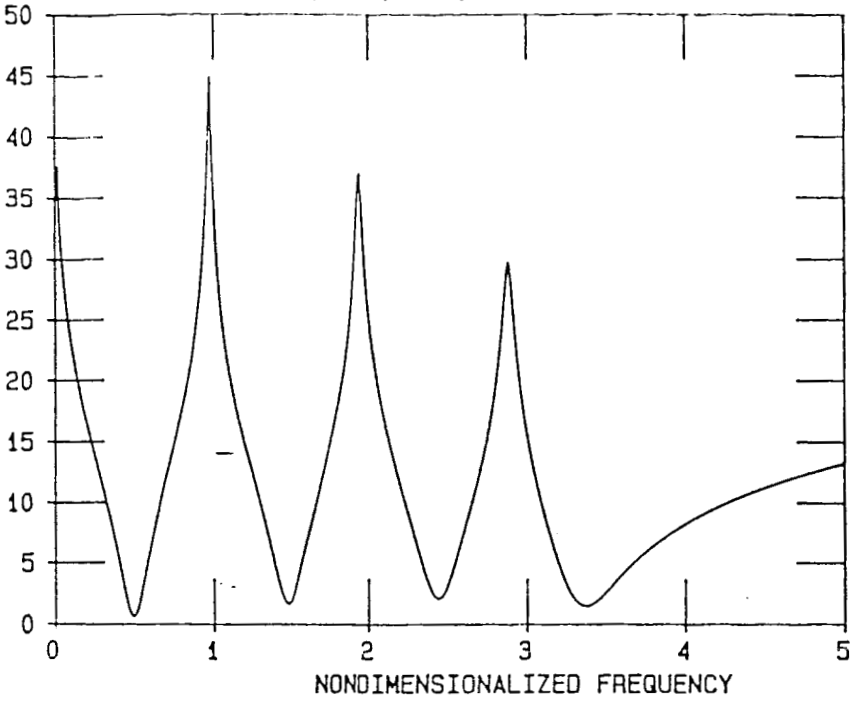

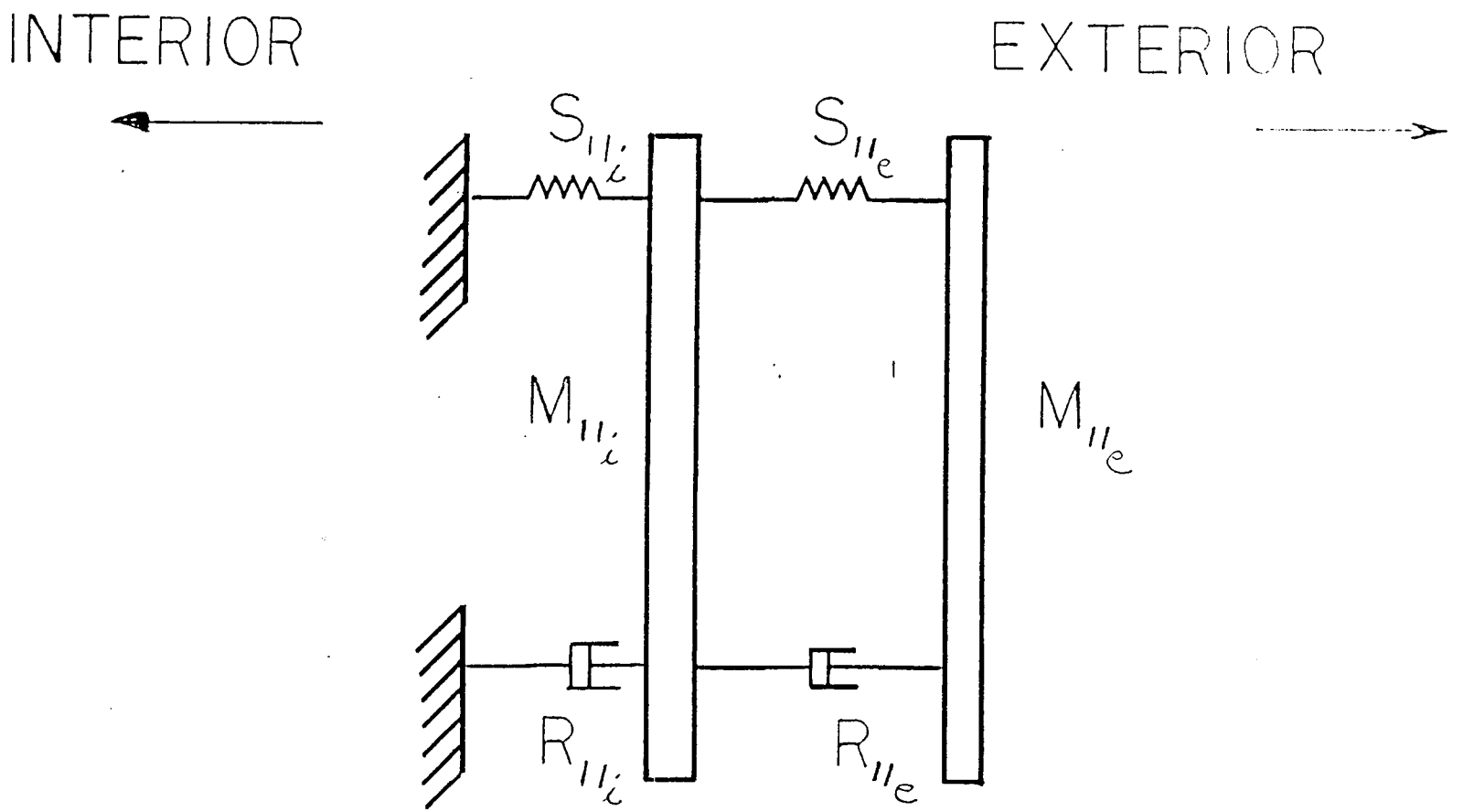

FIGURE 9: Individual Double Panel Section

SECTION 3. EXPERIMENTAL PROGRAM

A series of benchtop experiments have confirmed the potential of Alternate Resonance Tuning. A typical setup is shown in Figure 10. The ART panels are passively driven modified audio speakers of 4" diameter. A frequency generator drives a speaker system with a pure tone. A sound level measurement is first taken at point (1) (equivalent to the aircraft exterior). A second sound level measurement is taken at point (2) within the duct (the aircraft interior). The two sound pressure levels are differenced to provide a transmission loss or gain. The reflection condition at the other end of the duct can be varied from approximately anechoic to a hard wall condition. Three ducts have been constructed with ART panel arrays as shown in Figure 11. The duct dimensions as shown in Table 1 summarize the lettered dimensions shown in Figures 10 and 11.

In order to tune the resonances of the passive audio speakers which serve as ART panels, some time was spent modifying the speakers to achieve the desired resonant frequencies. Resonant frequencies were lowered by addition of mass to the speaker cones. On the other hand, resonant frequencies were raised by stiffening the speaker suspensions with epoxy. Methods were developed to determine the speaker masses, damping ratio, mechanical resistances, and spring constants. The voice coil EMF generated by the speakers provides a monitoring signal for analysis purposes.

Some typical experimental results are shown in Figures 12-15. Figure 12 shows the out of phase behavior of two ART speakers with resonances of 100 and 300 Hz. Note the relatively flat region of nearly out of phase behavior between 120 and 250 Hz. Figure 13a shows transmission loss across two identical speakers in the two panel duct with an anechoic termination. No transmission loss occurs at 200 Hz, the resonant frequency of these speakers.

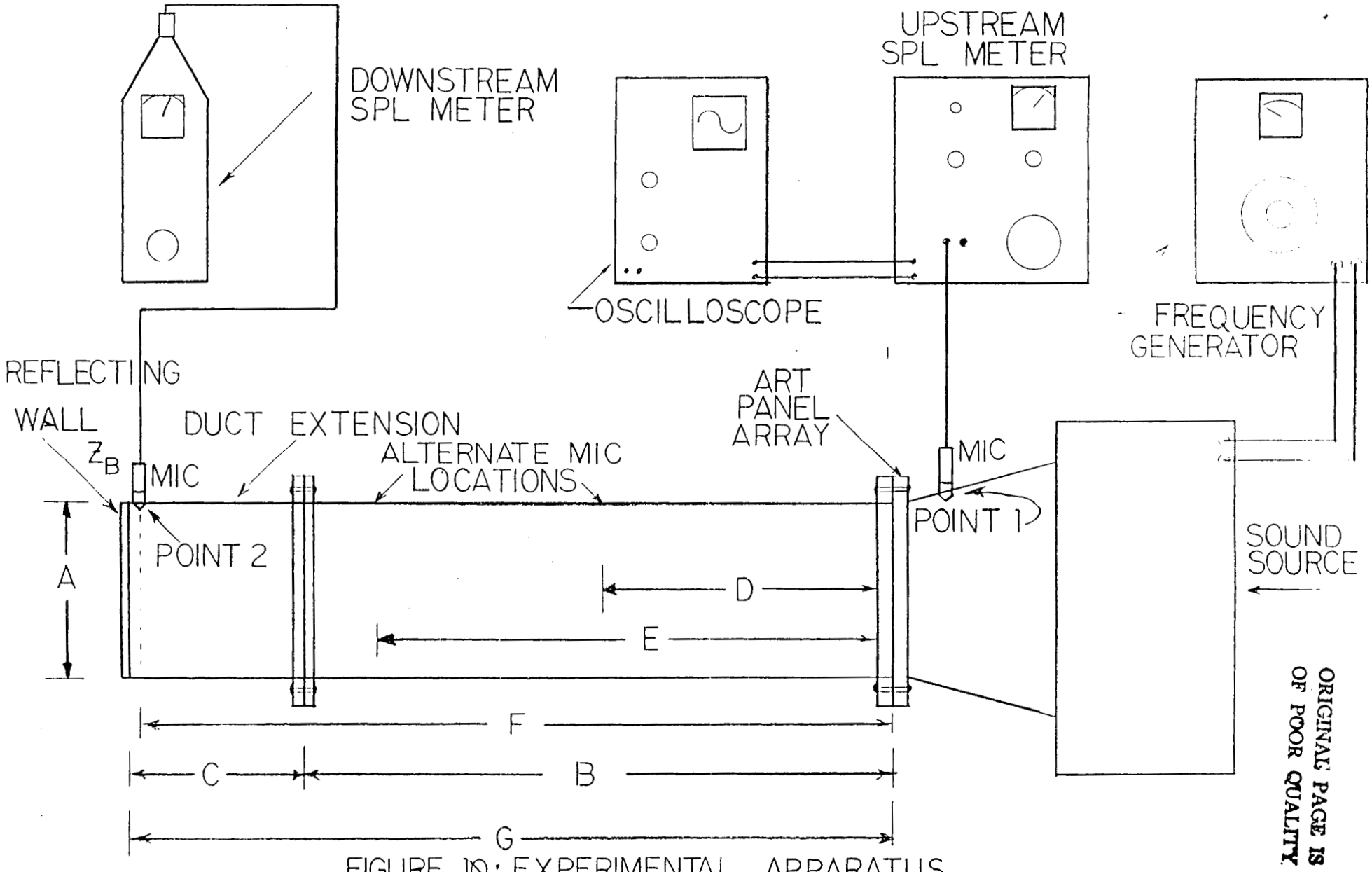

FIGURE 10: EXPERIMENTAL APPARATUS

FIGURE 11: ART PANEL ARRAYS

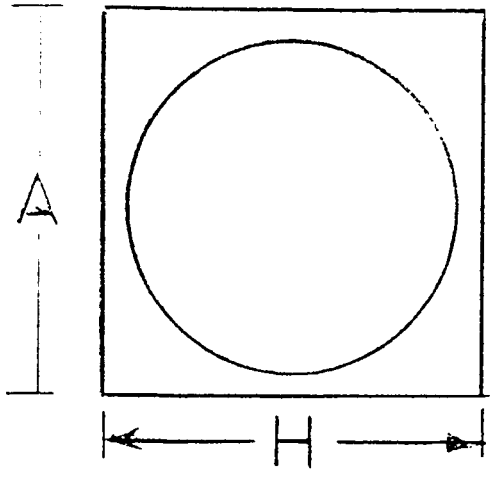

ONE SPEAKER

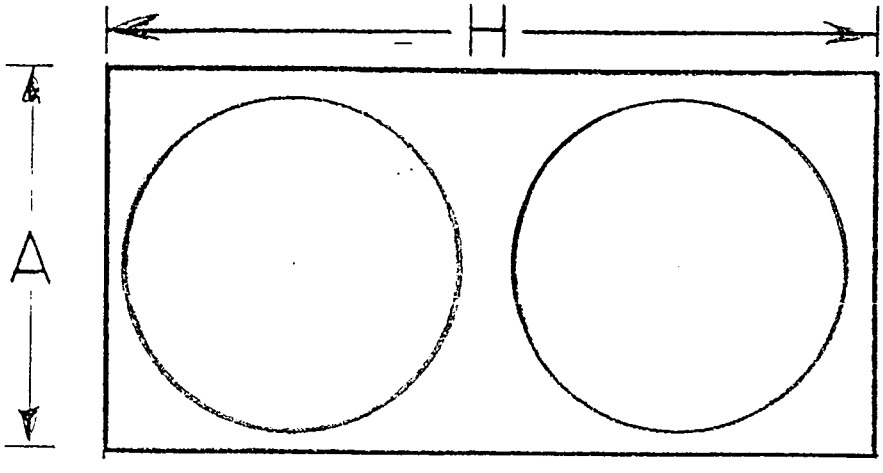

TWO SPEAKER

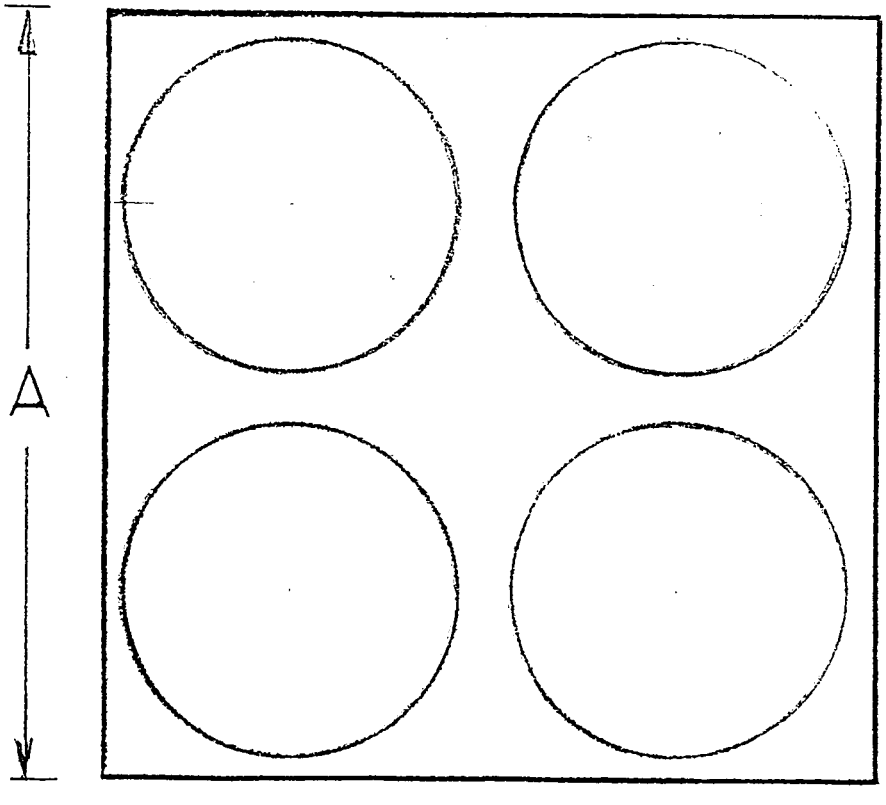

FOUR SPEAKER

TABLE 1 TYPICAL DUCT DIMENSIONS
REFER TO FIGURES 10 AND 11

DIMENSION DUCT	A	B	C	D	E	F	G	H
ONE SPEAKER	4.5"	67.5"	22.5"	43.5"	-	-	90.0"	4.25"
TWO SPEAKER	4.5"	67.0"	22.0"	42.5"	61.0"	83.0"	89.0"	8.25"
FOUR SPEAKER	8.5"	67.5"	22.5"	46.5"	63.0"	85.0"	90.0"	8.5"

FIGURE 12
PHASE DIFFERENCE BETWEEN ART SPEAKERS
RESONANT FREQUENCIES AT 100 AND 300 hz

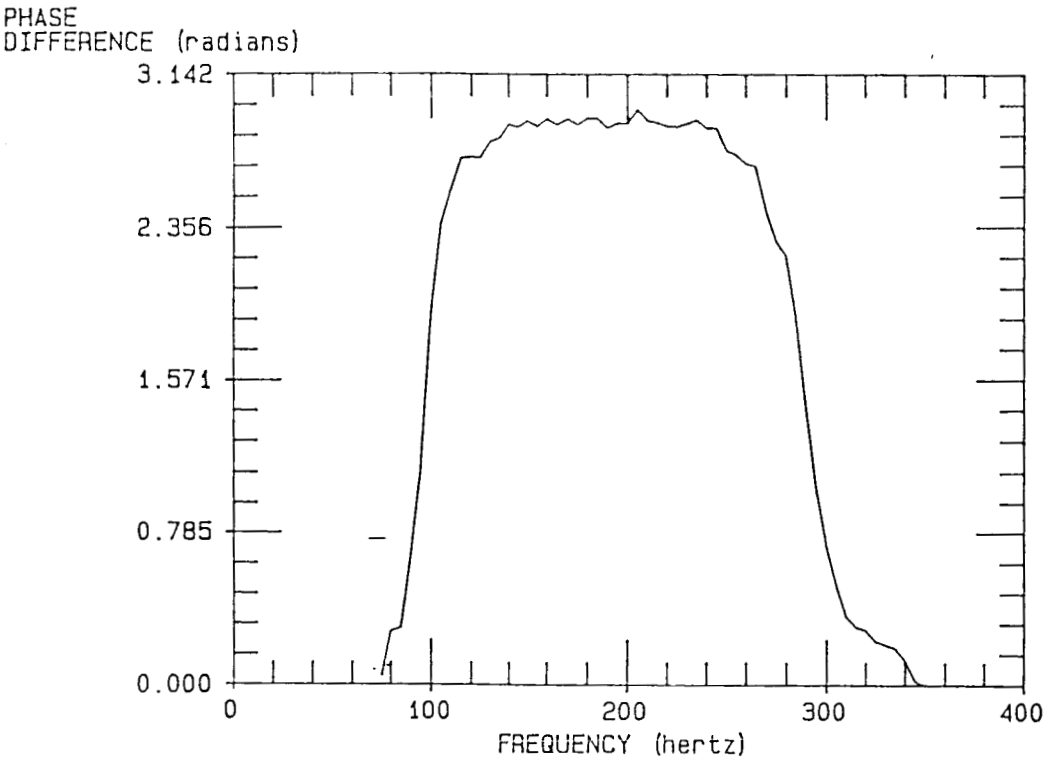

FIGURE 13A
TRANSMISSION LOSS ACROSS IDENTICAL SPEAKERS
RESONANT FREQUENCIES ARE 200 HERTZ
ANECHOIC TERMINATION

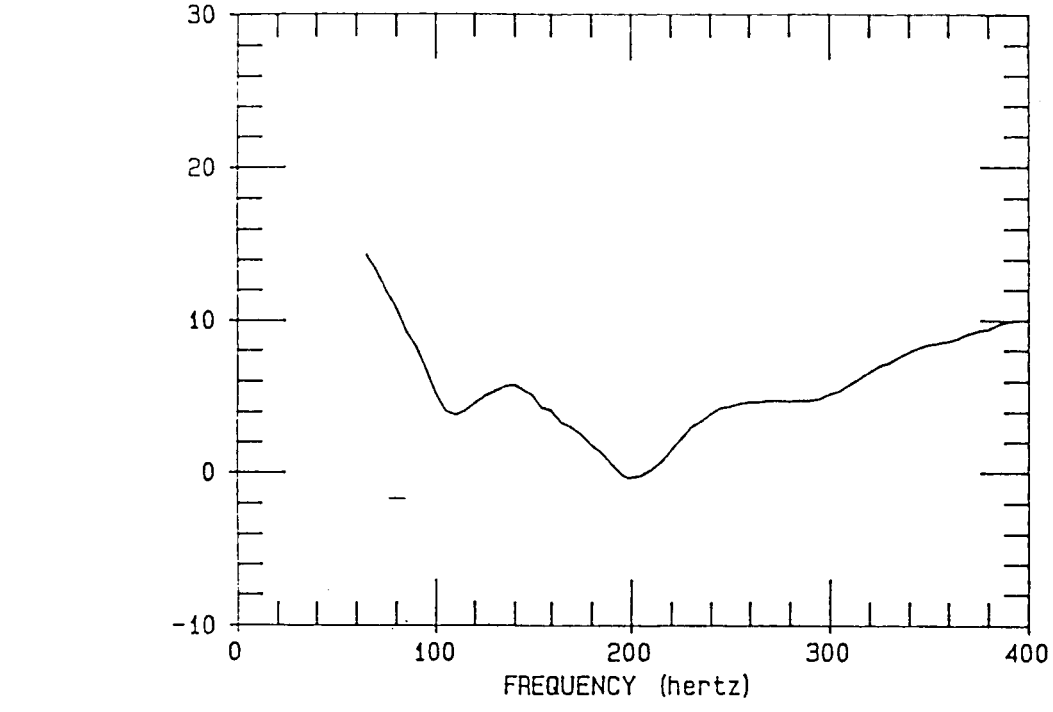

FIGURE 13B
TRANSMISSION LOSS ACROSS ART SPEAKERS
RESONANT FREQUENCIES ARE 100 AND 300 HERTZ
ANECHOIC TERMINATION

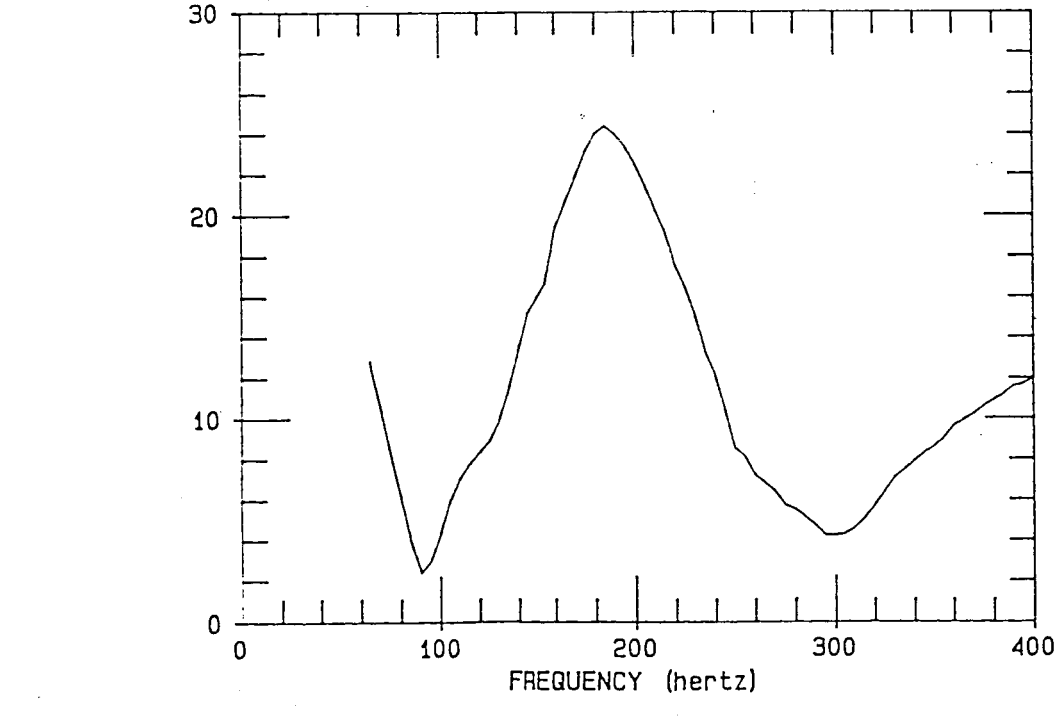

Figure 13b shows transmission loss across the ART speakers with resonances at 100 Hz and 300 Hz. Figure 13c plots the difference between the ART speakers and the identical speakers. This result shows that the ART panels are capable of attenuating sound more effectively than the identical panels.

Figures 13c, 13d and 13e show difference between ART data and identical speakers with different ART bandwidths. These figures show that a wider bandwidth between resonant frequencies results in increased transmission loss. As with the theoretical data presented in Section 2, an average transmission loss is calculated using equation (6) for the cases with resonances at 100/300 hertz, 200/300 Hz and 100/560 Hz. The difference between the ART data and the average transmission loss is shown in Figures 13f, 13g, and 13h. By increasing the bandwidth, the maximum difference between the ART data and average transmission loss data is increased to about 19 dB. Some experimentation has also been done with a double spring-mass-damper system (double SMD, Figure 9) resonating beside a single speaker in the two speaker duct. Figure 13i indicates a transmission loss of about 35 dB. This case is still being investigated.

Figure 14a shows four speakers with resonances at approximately 100, 200, 300, and 400 Hz in the four speaker duct. The three cancellation frequencies are very noticeable. Figure 14b shows transmission loss across four identical speakers with resonances at 200 Hz. Figure 14c shows the difference between the ART and identical speakers, and again three distinct cancellation peaks are indicated. It should be mentioned that the speaker parameters are not optimized at this point, and more attenuation could be achieved if these parameters were precisely set.

Figure 14d shows a transmission loss plot in the four panel duct with a

FIGURE 14A
TRANSMISSION LOSS ACROSS FOUR ART SPEAKERS
RESONANT FREQUENCIES AT 100, 200, 300, AND 400 HERTZ
ANECHOIC TERMINATION

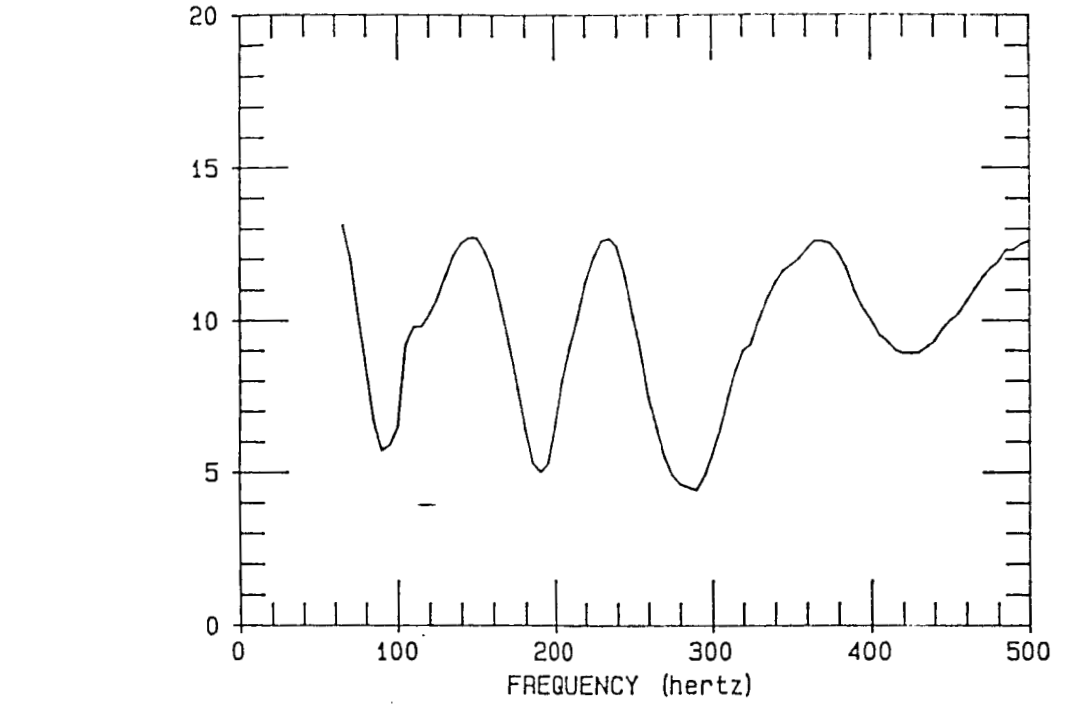

FIGURE 14B
TRANSMISSION LOSS WITH FOUR IDENTICAL SPEAKERS
WITH RESONANCES AT 200 HERTZ AND ANECHOIC TERMINATION

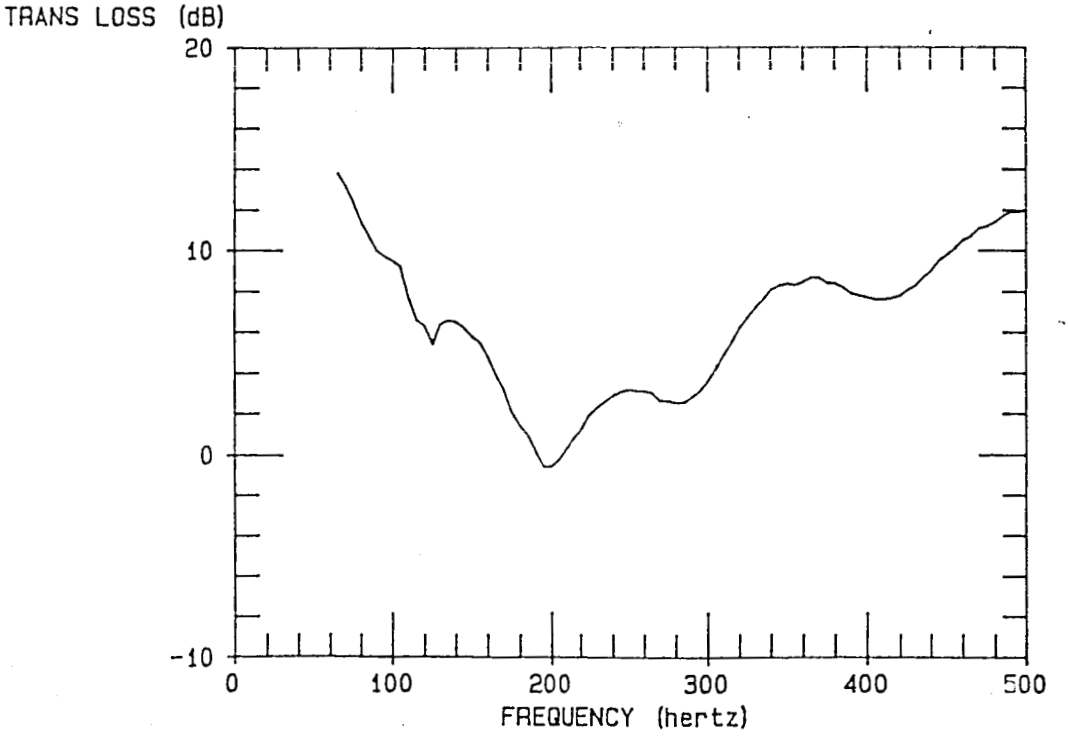

FIGURE 13C
DIFFERENCE BETWEEN ART AND IDENTICAL SPEAKER CASE
FOR SPEAKERS WITH RESONANCES AT 100 AND 300 HERTZ

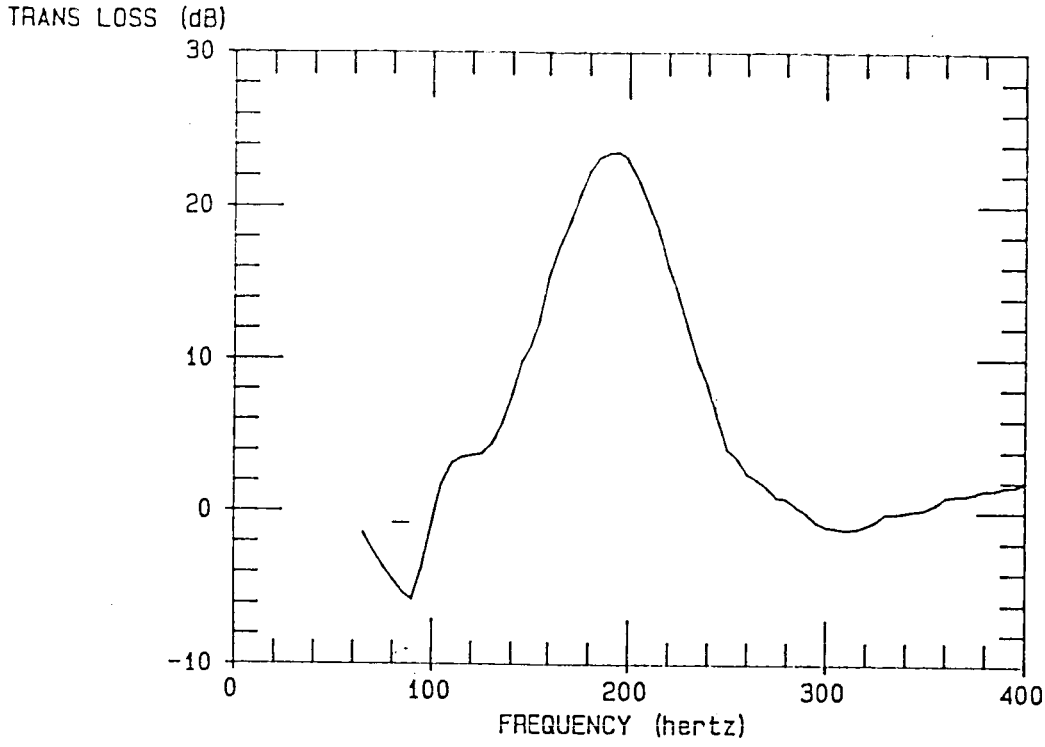

FIGURE 13D
DIFFERENCE BETWEEN ART AND IDENTICAL SPEAKER CASE
WITH SPEAKER RESONANCES AT 200 AND 300 HERTZ AND
ANECHOIC TERMINATION

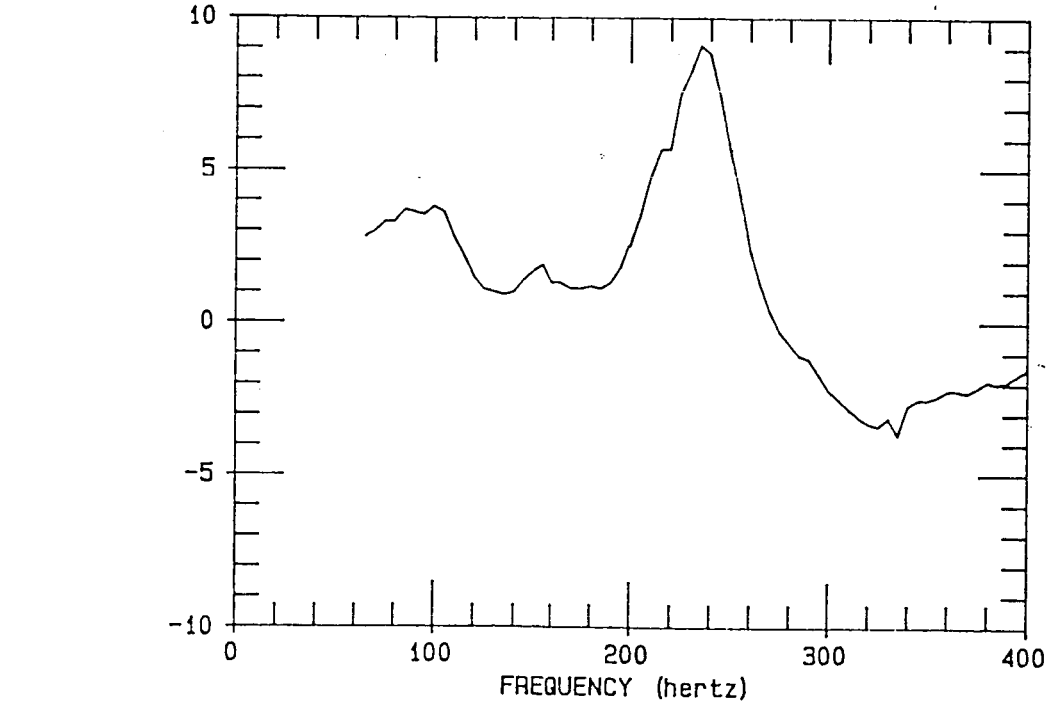

FIGURE 13E
DIFFERENCE BETWEEN ART AND IDENTICAL SPEAKER CASE WITH SPEAKER RESONANCES AT 100 AND 570 HERTZ AND ANECHOIC TERMINATION

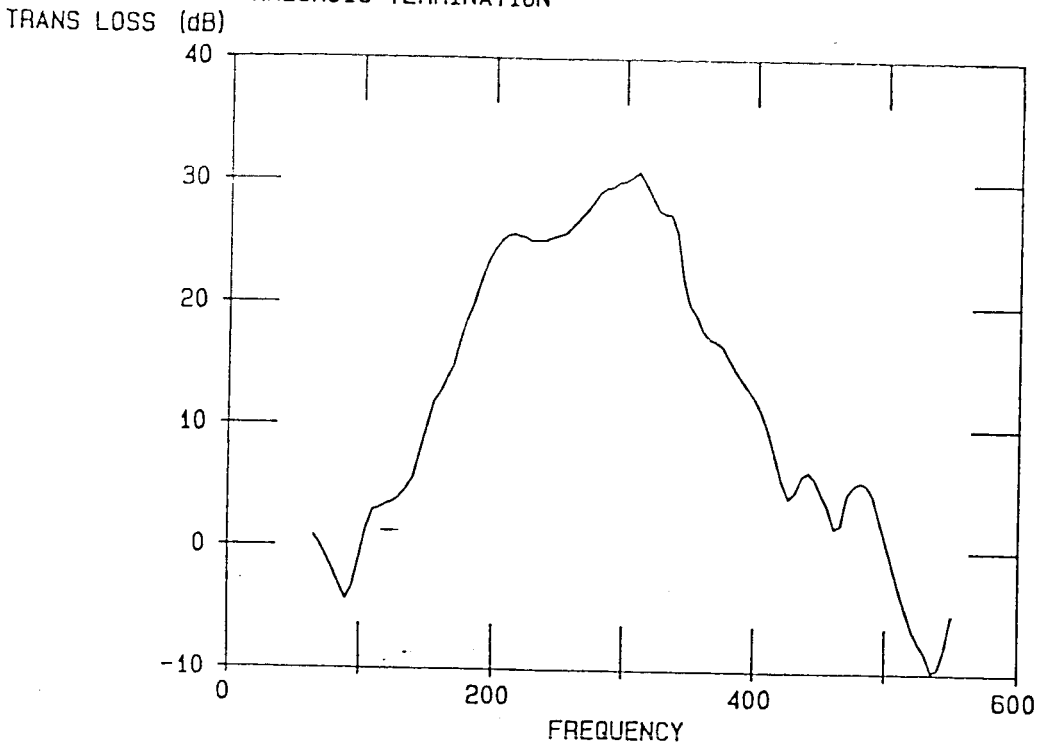

FIGURE 13F
DIFFERENCE BETWEEN ART AND AVERAGE TRANSMISSION LOSS FOR SPEAKERS WITH RESONANCES AT 100 AND 300 HERTZ

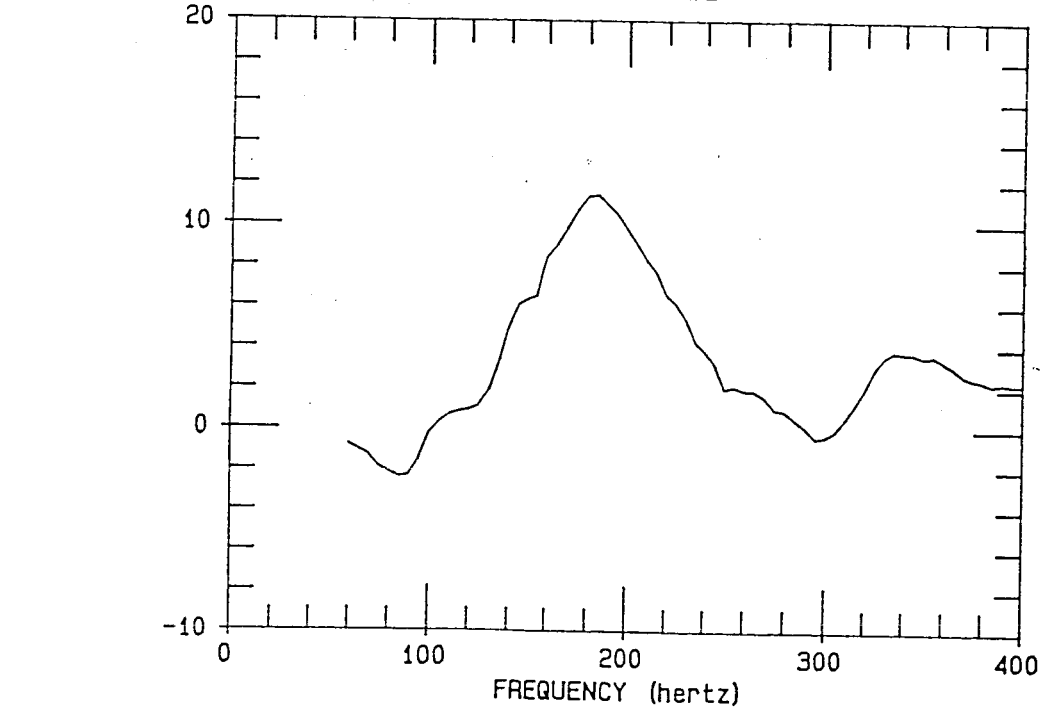

FIGURE 13G
DIFFERENCE BETWEEN ART DATA AND AVERAGE
TRANSMISSION LOSS FOR SPEAKERS WITH
RESONANCES AT 200 AND 300 HERTZ

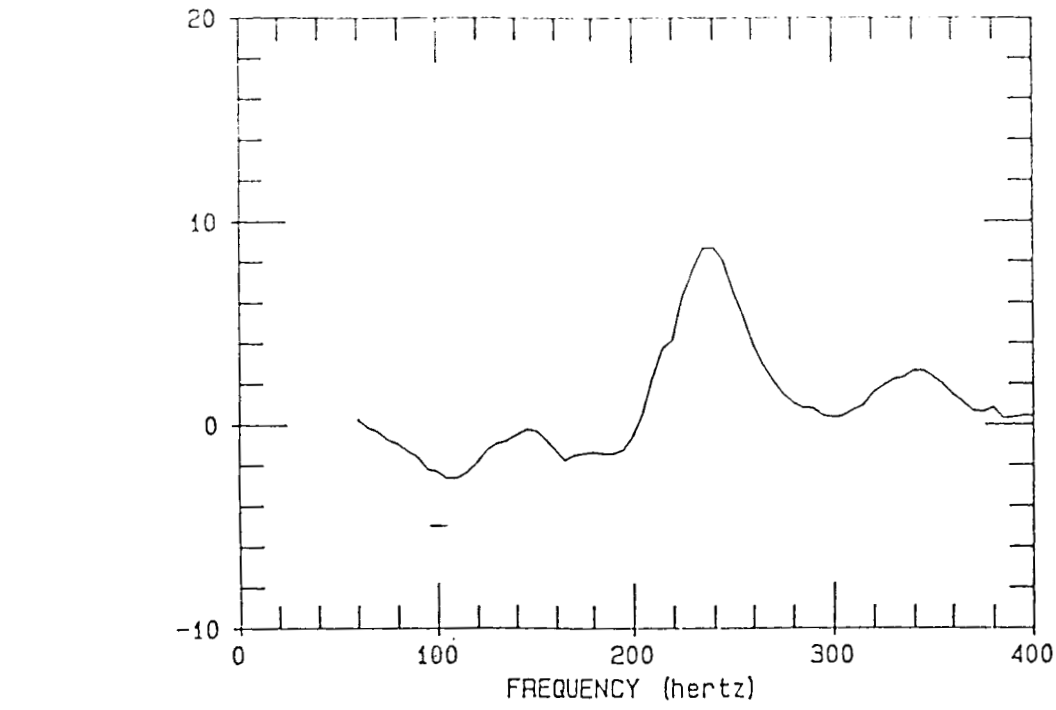

FIGURE 13H
DIFFERENCE BETWEEN ART DATA AND AVERAGE
TRANSMISSION LOSS FOR SPEAKERS WITH
RESONANCES AT 100 AND 560 HERTZ.

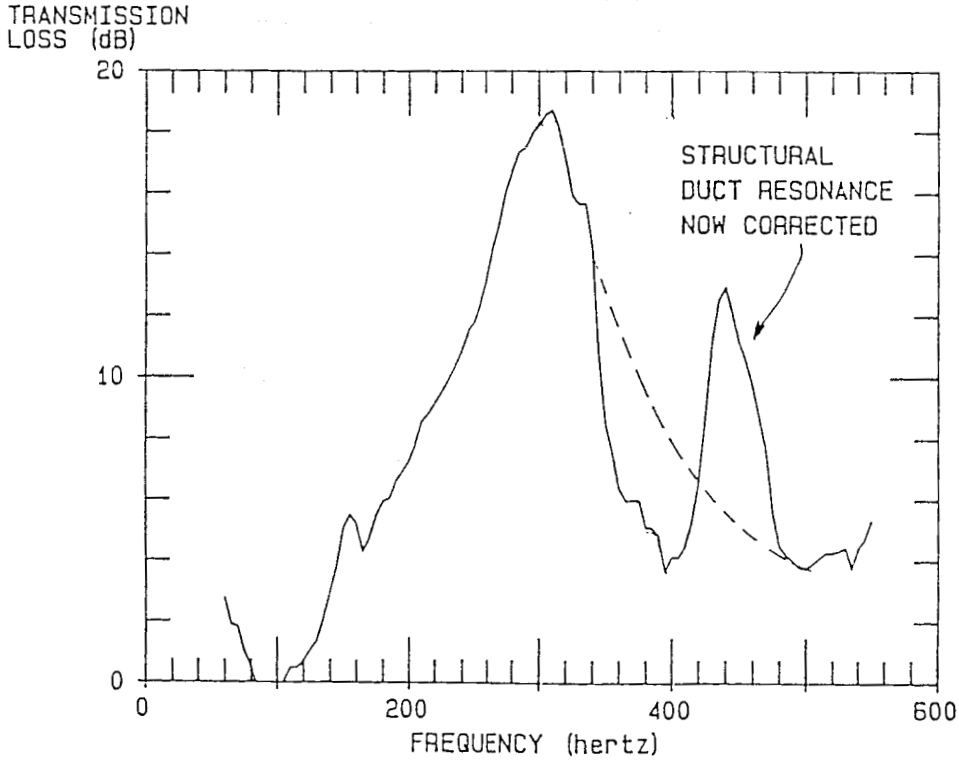

FIGURE 13I
TRANSMISSION LOSS ACROSS ART SPEAKERS
DOUBLE SMD SYSTEM WITH RESONANCES OF 68 hz AND
SINGLE SMD SYSTEM WITH A RESONANCE OF 560 hz.
ANECHOIC TERMINATION

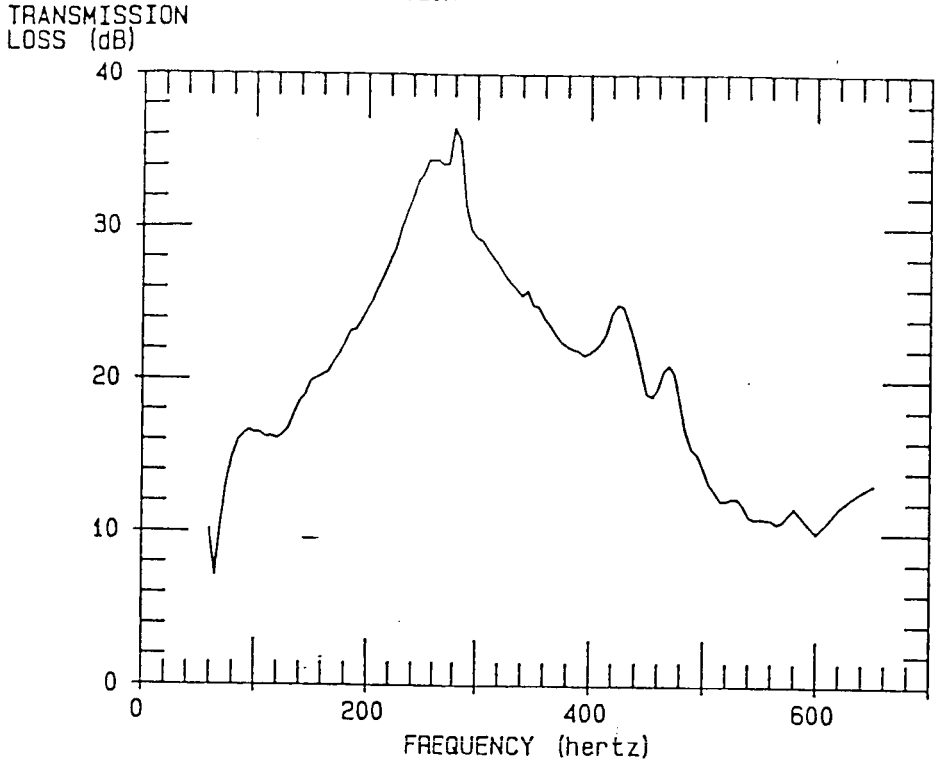

FIGURE 14C
DIFFERENCE BETWEEN ART AND IDENTICAL SPEAKER CASE
FOUR SPEAKER DUCT WITH ANECHOIC TERMINATION AND SPEAKER
RESONANCES AT 100, 200, 300, AND 400 HERTZ

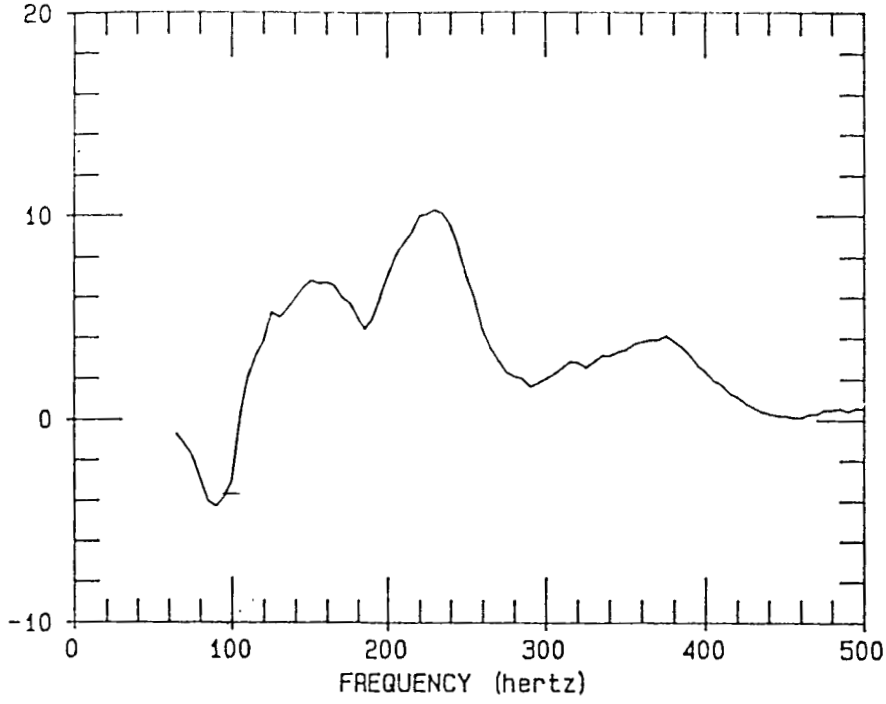

FIGURE 14D
TRANSMISSION LOSS ACROSS FOUR ART SPEAKERS
RESONANT FREQUENCIES AT 100, 200, 300, AND 400 HERTZ
REFLECTING WALL NORMALIZED IMPEDANCE = 9.3 AT 200 HERTZ (α=.35)

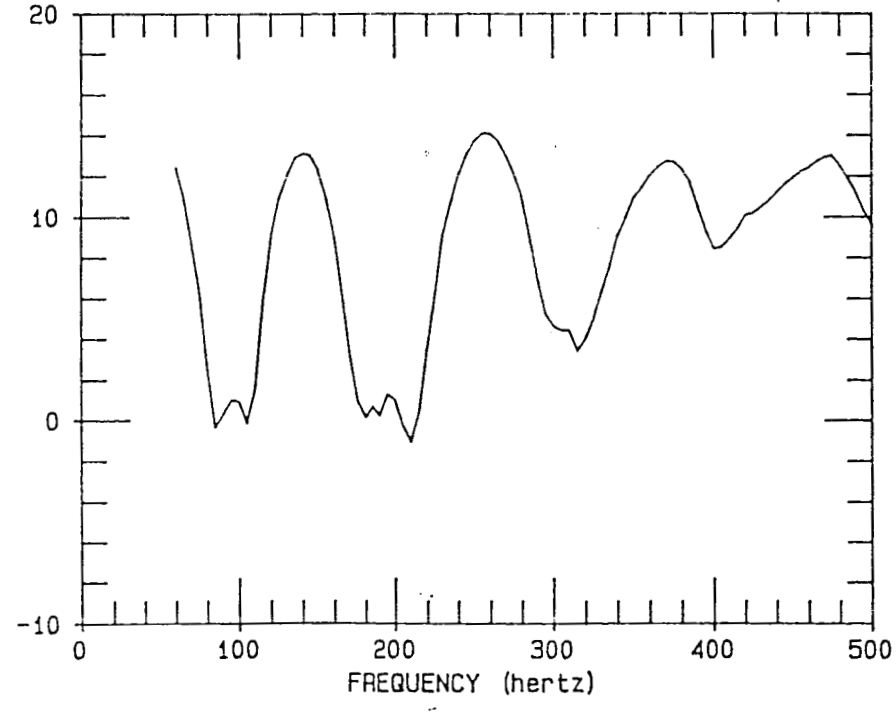

reflecting wall absorption coefficient α = .35 (corresponding to an acoustic modal damping ζ = ≈ .03). Three cancellation peaks are shown with a maximum attenuation of 13 dB. This result demonstrates that the ART principle can work well in the presence of wall reflections.

In the months to come, more work will proceed with general ART two and four speaker transmission loss experiments. A flexible frame model is being developed to determine if a vibrating fuselage frame can play a favorable role in ART transmission loss. We are also preceding with near field fall-off measurements inside the duct to further quantify ART effectiveness near the panel wall.